공학석사학위논문

Fluoride and Bacteriophage MS2 Removal from Aqueous Solution Using Pyrophyllite as Adsorbents

납석을 흡착제로 이용한 수용액상의
불소와 박테리오파지 MS2 제거

2013 년 2 월

서울대학교 대학원

생태조경 · 지역시스템공학부

지역시스템공학전공

김 재 현

Fluoride and Bacteriophage MS2 Removal from Aqueous Solution Using Pyrophyllite as Adsorbents

납석을 흡착제로 이용한 수용액상의
불소와 박테리오파지 MS2 제거

지도교수 김 성 배
이 논문을 공학석사 학위논문으로 제출함

2012년 12월

서울대학교 대학원
생태조경·지역시스템공학부
지역시스템공학전공

김 재 현

김 재 현 의 공학석사 학위논문을 인준함.
2013년 1월

위 원 장 _____ (인)

부위원장 _____ (인)

위 원 _____ (인)

Fluoride and Bacteriophage MS2 Removal from Aqueous Solution Using Pyrophyllite as Adsorbents

A THESIS
SUBMITTED TO THE DEPARTMENT OF LANDSCAPE
ARCHITECTURE AND RURAL SYSTEMS ENGINEERING
AND THE COMMITTEE ON GRADUATE STUDIES
OF SEOUL NATIONAL UNIVERSITY
IN PARTIAL FULFILLMENT OF THE REQUIREMENTS
FOR THE DEGREE OF

MASTER OF ENGINEERING

By

JAE-HYUN KIM

FEBRUARY, 2013

I certify that I have read this thesis and that in my opinion it is fully adequate, in scope and quality, as thesis for the degree of Master of Engineering.

_____

Chair of Committee

I certify that I have read this thesis and that in my opinion it is fully adequate, in scope and quality, as thesis for the degree of Master of Engineering.

_____

Vice-Chair of Committee

I certify that I have read this thesis and that in my opinion it is fully adequate, in scope and quality, as thesis for the degree of Master of Engineering.

_____

Member

Abstract

The objective of this study is to investigate the removal of fluoride and bacteriophage from aqueous solution using pyrophyllite as adsorbents. Pyrophyllite particles used in the experiments are white with rough and heterogeneous surfaces. The chemical composition from X-ray fluorescence (XRF) analysis showed that the major constituents of pyrophyllite were Si (74.03%) and Al (21.20%). The X-ray diffraction (XRD) pattern indicated peaks for quartz (SiO_2), dickite ($Al_2Si_2O_5(OH)_4$), and pyrophyllite ($Al_2Si_4O_{10}(OH)_2$). In the Fourier transform infrared (FTIR) spectra, a band recorded at 3652 (1/cm) corresponded to O-H stretching vibrations for OH groups bonded to Al ions. A band at 938 (1/cm) was attributed to OH bending vibrations for Al-OH groups. N_2 adsorption-desorption analysis indicated that BET surface area of pyrophyllite was 1.3419 m^2/g with total pore volume of 5.74×10^{-4} cm^3/g and average pore diameter of 1.7122 nm.

Equilibrium test (adsorbent particle size < 0.15 mm) demonstrated that the maximum sorption capacity of pyrophyllite was 0.737 mg/g. Kinetic test showed that fluoride sorption to pyrophyllite arrived at equilibrium around 24 h. Thermodynamic test indicated that fluoride sorption to pyrophyllite increased with increasing temperature from 25 to 45 ^oC, indicating the endothermic nature of sorption process. Further experiments indicated that fluoride removal was not sensitive to solution pH between 4.0 and 9.0. The influence of sulfate, carbonate, and phosphate on the removal of fluoride was important while the effect of nitrate

and chloride was negligible. In addition, among the pyrophyllite thermally treated at different temperatures (untreated, 400, 600, 800, 1000, 1100 ^{o}C), the adsorbent treated at 400 ^{o}C had the highest adsorption capacity (21% higher than that of untreated pyrophyllite).

Batch and column experiments were also conducted to examine the MS2 sorption on pyrophyllite. Results demonstrated that pyrophyllite was effective in removing MS2. The percent removal of MS2 increased from 5.26 to 99.99% with increasing pyrophyllite doses from 0.01 to 1.0 g per 30 mL solution (initial MS2 concentration = 2.85×10^6 pfu/mL). The maximum removal capacity of pyrophyllite for MS2 was determined to be 5.01×10^8 pfu/g. The sorption of MS2 to pyrophyllite was a fast process with 3.7 log removal within 30 min and more than 4.0 log removal after 180 min. The influence of fluoride on the removal of MS2 on pyrophyllite was observed under batch conditions. At fluoride concentrations of 5 and 10 mg/L, the log removals of MS2 on pyrophyllite were 3.05 and 2.54, respectively, which were lower than that with no fluoride present (4.0 log removal). Results suggested that the removal of MS2 on pyrophyllite was influenced by fluoride ions because fluoride ions could compete with MS2 for sorption sites on the pyrophyllite surface. Column results showed that pyrophyllite was effective in removing MS2 under flow-through conditions (flow rate = 0.5 mL/min; initial MS2 concentration = 5.98×10^5 pfu/mL), with a removal capacity of 8.17×10^6 pfu/g with no fluoride present and 4.70×10^6 pfu/g with 5 mg/L fluoride present. The effect of fluoride on MS2 removal in column experiments was not as substantial as the effects in the batch

experiments under the given conditions. This study demonstrates that pyrophyllite clay could be used as an adsorbent for the removal of fluoride and viruses from water.

Keywords: adsorbent, bacteriophage MS2, batch experiment, clay, column experiment, fluoride, pyrophyllite, sorption, thermodynamic experiment

Contents

List of Tables

List of Figures

I. Introduction

1. Background

Pyrophyllite is a 2:1 clay mineral having dioctahedral layer structure with octahedrally coordinated Al ion sheets between two sheets of SiO_4 tetrahedra (Figure 1-1). It belongs to the family of silicate minerals that are composed of three infinite layers formed by the sharing of oxygen ions at three corners of the silica tetrahedral. A layer of octahedrally coordinated Al-OH ions holds the two layers of tetrahedrally coordinated Si-O ions together as a three-layer sheet (Gücek et al., 2005). It is a hydrous aluminosilicate clay with the chemical composition $Al_2Si_4O_{10}(OH)_2$ (Bentayeb et al., 2003). The primary countries producing pyrophyllite are located in northeast Asia and include China, Korea, and Japan. Pyrophyllite has many industrial applications, including as a raw material in the ceramic, glass, and refractory industries (Indian Bureau of Mines, 2011). Pyrophyllite has recently been investigated as a potential low-cost and environmental friendly adsorbent for removing contaminants such as boron, cyanide, fluoride, heavy metals and dyes from water and wastewater (Keren and Sparks, 1994; Saxena et al., 2001; Gücek et al., 2005; Prasada and Saxena, 2008; Gupta et al., 2009; Goswami and Pukait, 2011).

Fluoride contamination in drinking water resources is a serious environmental problem around the world. In many countries such as India, China, The Middle East, and African countries, fluoride occurs naturally in groundwater at concentrations exceeding the guidelines of the World Health Organization (1.5 mg/L), causing

serious health problems. Above 1.5 mg/L fluoride could cause neurological damages and dental/skeletal fluorosis (Ayoob and Gupta, 2006). In addition, the viral contamination of groundwater resources is a serious problem that can result in outbreaks of waterborne disease. Such viral contamination may originate due to septic tank effluents, land application of wastewater, private waste-disposal system, and municipal sanitary landfills (Yates et al., 1985). Consequently, these lead to degradation in a drinking water quality and a threat to public health (Bosch et al., 2008).

To provide safe drinking water, adsorption is widely used mainly because of cost effectiveness and simplicity of operation. Various adsorbents have been used for fluoride removal and preventing waterborne viral diseases, including activated alumina, activated carbon, granular ferric hydroxide, activated carbon, bituminous coal, and so on. However, very limited studies have been conducted for the application of pyrophyllite to fluoride and virus removal, though fluoride and virus are one of the major groundwater contaminant.

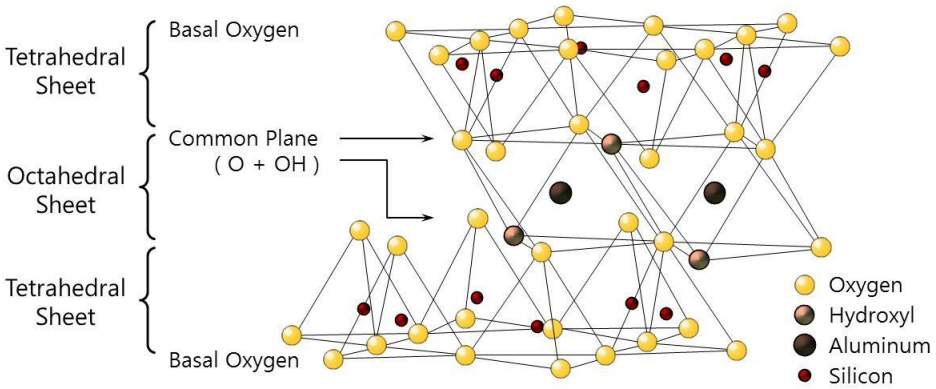

Figure 1-1. Schematic drawing of pyrophyllite structure.

2. Objectives

The objective of this study is to investigate the removal of fluoride and bacteriophage MS2 from aqueous solution using pyrophyllite as adsorbents.

3. Method of approach

The characteristics of pyrophyllite were elucidated using X-ray fluorescence (XRF) spectrometer, X-ray diffraction (XRD) spectrometer, field emission scanning electron microscopy (FESEM) and Fourier transform infrared (FTIR) spectrometer. Equilibrium, kinetic, and thermodynamic experiments were performed to examine the adsorption of fluoride to pyrophyllite. Batch experiments were also conducted to observe the removal of MS2 by pyrophyllite. In addition, the influence of fluoride on the removal of MS2 on pyrophyllite was observed under batch conditions. Flow-through column experiments were performed in pyrophyllite columns to examine the removal of MS2 in both the absence and presence of fluoride.

II. Literature Review

1. Adsorption of fluoride on clays

For the removal of fluoride from water, adsorption is widely used mainly because of cost-effectiveness and simplicity of operation. Various adsorbents have been used for fluoride removal, including activated alumina, activated carbon, granular ferric hydroxide, limestone, fly ash, etc. (Bhatnagar et al., 2011). These materials may be limited their use as an adsorbent due to the cost constraint or unsatisfactory level of fluoride ion adsorption capacity (Goswami and Purkait, 2011). Clays have also been considered as alternative adsorbents with great potential because of their large quantities, chemical and mechanical stability, high surface area, and structural properties (Chen and Wang, 2007). When compared with other low-cost adsorbents, clays have been found to be either better or equivalent in contaminant adsorption capacity from water (Srinivasan, 2011). The use of clays to remove fluoride has been investigated by several researchers (Bhatnagar et al., 2011). Chaturvedi et al (1988) examined the adsorption of fluoride to china clay. They showed that the alumina constituent of china clay is responsible for maximum adsorption of fluoride in the pH range of interest. Kau et al (1998) studied fluoride sorption behavior by kaolinite and bentonite. They determined that bentonite was superior fluoride sorbent than kaolinite quantitatively, although experimental results had suggested that fluoride sorption by bentonite may not be achieved through the same sorption mechanism as for kaolinite. Karthikeyan et al (2005) investigated fluoride removal by montmorillonite under various contact times and temperatures. They reported

that montmorillonite exhibited an increase in the adsorption rate at higher temperatures and the adsorption is endothermic.

2. Adsorption of virus on clays

Clays have also been tested for virus removal because of their large surface area and high ion exchange capacity (Moore et al., 1981, 1982; Lipson and Stotzky, 1982; Schiffenbauer and Stotzky, 1982, 1983; Lipson and Stotzky, 1985; Sobsey et al., 1986). Sykes and Williams (1978) investigated the adsorption of phages (f6, f13) on the three clays including light clay kaolin, calcium montmorillonite, and sodium montmorillonite. This work demonstrated that kaolin adsorbed more phage than montmorillonite and adsorption to the former was greater when it was unsubstituted or homoionized with Na^{+} than when it was treated with Ca^{2+} or Al^{3+}. Taylor et al (1980) described the interactions of bacteriophage R17 and reovirus type 3 by the amorphous aluminosilicate clay mineral allophane. They showed that allophane exhibited a strong affinity for both bacteriophage R17 and reovirus over the pH range 5-7, the natural pH range of many fresh waters. Sobsey et al (1980) studied the adsorption of viruses (poliovirus, reovirus) on different soil materials. The results showed that clays were more efficient in the removal of enteric viruses from wastewater than sand or organic soil. Chattopadhyay and Puls (1999) performed thermodynamic studies of the adsorption of bacteriophages (MS2, PhiX174, T2) on clay adsorbents including hectorite, kaolinite, and saponite. The authors reported that sorption was dependent on the surface hydrophobicity of both adsorbents and bacteriophages.

3. Adsorption of contaminants on pyrophyllite

A number of studies have recently explored pyrophyllite as potential adsorbent for various contaminants from water and wastewater. Keren and Sparks (1994) examined the effect of pH and ionic strength on boron adsorption by pyrophyllite. They observed that boron adsorption by pyrophyllite at pH 7 was lower than the amount of adsorbed at pH 9 and boron adsorption increased with increasing ionic strength. Saxena et al (2001) studied the adsorption of cyanide by pyrophyllite. They showed the effect of initial concentration of adsorbate, amount of adsorbent, pH and temperature of test solutions. Gücek et al (2005) described the adsorption of cationic dye (methylene blue) and anionic dye (procion crimson H-EXL) from aqueous medium on pyrophyllite. They reported that nearby 2 min of contact time were found to be sufficient for the adsorption of both dyes to reach equilibrium and pyrophyllite could used as low-cost adsorbent for removing both cationic and anionic dyes. Prasad and Saxena (2008) investigated sericitic pyrophyllite as an adsorbent for the possible application in the removal of divalnt toxic cations such as Pb^{2+}, Cu^{2+}, and Zn^{2+}. They demonstrated that the adsorption process was found to be endothermic and the Freundlich adsorption model was found to represent the experimental results at different temperatures more suitably. Also Gupta et al (2009) modeled and simulated to predict kinetic parameters for the adsorption of Pb^{2+}, Cu^{2+}, Zn^{2+} onto pyrophyllite. Goswami and Purkait (2011) carried out batch adsorption study to remove excess fluoride from water using pyropyllite.

Table 2-1. Previous studies for fluoride removal from water using clay minerals.

Author	Title	Adsorbent	Summary
Chaturvedi et al (1988)	Fluoride removal from water by adsorption on china clay	China clay	The results indicate that under suitable conditions, china clay may be used as a potential adsorbent for the removal of fluoride from water.
Kau et al (1998)	Experimental sorption of fluoride by kaolinite and bentonite	Kaolinite, Bentonite	The results indicate that the single most important factor affecting fluoride sorption on clay is the solution pH.
Srimurali et al (1998)	A study on removal of fluorides from drinking water by adsorption onto low-cost materials	Various low-cost materials including bentonite, Kaolinite, Iignite	At optimum system conditions, bentonite exhibited highest removal capacity.
Karthikeyan et al (2005)	Fluoride adsorption studies of montmorillonite clay	Montmorillonite	Montmorillonite exhibits an increase in the adsorption rate at higher temperatures and follows endothermic process.
Tor (2006)	Removal of fluoride from an aqueous solution by using montmorillonite	Montmorillonite	The study investigated the fluoride uptake for montmorillonite under different physical and chemical conditions and dertermined the best fit adsorption isotherm.

Table 2-1. (Continued).

Author	Title	Adsorbent	Summary
Hamdi and Srasra (2007)	Removal of fluoride from acidic wastewater by clay mineral: Effect of solid-liquid ratios	Tunisian clays	Solution pH governs the amount of variable charge on the clay and also the extent to which hydroxyl groups may be removed to facilitate fluoride sorption process.
Meenakshi et al (2008)	Enhanced fluoride sorption by mechanochemically activated kaolinites	Kaolinite	The results indicate micronized kaolinite activated mechanochemically is cheap, indigenous, and eco-friendly material and could be employed as a low cost defluoridating agent.
Ramdani et al (2010)	Removal of excess fluoride ions from Sahara brackish water by adsorption on natural materials	Algerian clay (Montmorillonite with and without calcium)	The results suggested that montmorillonite without calcium, which was activated chemically and thermally was more efficient for defluoridation of brackish groundwater.
Goswami and Purkait (2011)	Kinetic and equilibrium study for the fluoride adsorption using pyrophyllite	Pyrophyllite	Through batch experiments, pyrophyllite showed significant fluoride removal efficiency at pH 4.9 and had considerable potential for fluoride removal from aqueous solution.

Table 2-2. Previous studies for viral removal from water using clay minerals.

Author	Title	Adsorbent	Virus	Summary
Bartell et al (1960)	The adsorption of enteroviruses by activated attapulgite	Claysorb	Poliovirus, Ecoviruses, etc	The results suggested a potential use for claysorb in localized intestinal in infections and other syndromes associated with enteroviruses.
Carlson et al (1968)	Virus inactivation on clay particles in natural waters	Kaolinite, Montmorillonite, Illite	T2, Poliovirus 1	The primary influencing factor of the added cations was that of effecting a proper charge distribution leading to a clay-cation-virus bridge, whereupon the virus was removed along with the removal of clay.
Sykes and Williams (1978)	Interactions of actibophage and clays	Light kaolin, Calcium montmorillonite, Sodium montmorillonite	f6, f13	Kaolin adsorbed more phage than montmorillonite and adsorption to kaolin was not influenced by pH and most of the adsorbed phage retained their infectivity.
Babich and Stotzky (1980)	Reductions in inactivation rates of bacteriophages by clay minerals in lake water	Kaolinite, Montmorillonite, Attapulgite	T1, P1, Qβ, 80α, pi11M15	Differences were noted in the rate of inactivation of bacteriophages in natural lake water, with the sequence of lability being pi11M15 > *Q*β > 8α > P1 > T1.

Table 2-2. (Continued).

Author	Title	Adsorbent	Virus	Summary
Taylor et al (1980)	Interaction of bacteriophage r17 and reovirus type III with the clay mineral allophane	Allophane, Montmorillonite	r17, reovirus type III	The principal factors influencing adsorption were found to be mixing time, pH and the concentrations and isoelectric points of both the virus and the absorbent.
Moore et al (1981)	Poliovirus adsorption by 34 minerals and soils	Soils, Minerals, and other substrates	Poliovirus 2	The most effective adsorbents were magnetite sand and hematite, which are predominantly oxides of iron.
Moore et al (1982)	Adsorption of reovirus by minerals and soils	Dry soils, Minerals and groundrocks	Reovirus	All of the minerals and soils studied were excellent adsorbents of reovirus, with greather than 99% of the virus adsorbed after 1h at 4°C.
Schiffenbauer and Stotzky (1982)	Adsorption of coliphages T1 and T7 to clay minerals	Kaolinite, Montmorillonite	T1, T7	Maximum adsorption of T7 to M was greater than that of T1, but adsorption to K was the same.
Lipson and Stotzky (1983)	Adsorption of reovirus to clay minerals: effects of cation-exchange capacity, cation saturation, and surface area	Kaolinite, Montmorillonite	Reovirus 3	The sequence of the amount of adsorption to homoionic montmorillonite was Al > Ca > Mg > Na > K; the sequence of adsorption to kaolinite was Na > Al > Ca > Mg > K.

Table 2-2. (Continued).

Author	Title	Adsorbent	Virus	Summary
Schiffenbauer and Stotzky (1983)	Adsorption of coliphages T1 and T7 to host and non-host microbes and to clay minerals	Kaolinite, Montmorillonite	T1, T7	Clays are more important than microbes as adsorbents of viruses in environments of low ionic strength and that microbes do not inactivate coliphages T1 and T7.
Lipson and Stotzky (1985)	Infectivity of reovirus adsorbed to homoionic and mixed-cation clays	Kaolinite, Montmorillonite	Reovirus 3	More virus was adsorbed by the clays, especially by K, below pH 4, indicating that electrostatic interactions occurred between the net negatively-charged clays and the net neutral or positively-charged virus.
Sobsey et al (1986)	Survival and transport of hepatitis A virus in soils, groundwater and wastewater	Bentonite, Kaolinite, Cecil clay loam, Ponzer organic muck, Flushing meadows loamy sand, Corolla coarse sand	Hepatitis A virus, Poliovirus type 1, Echovirus type 1	All three viruses were adsorbed relatively efficiently by clay soils, such as kaolinite clay and Cecil loam, and poorly by sandy soils and an organic muck.
Sobsey et al (1995)	Comparative reductions of hepatitis A virus, enteroviruses and coliphage MS2 in miniature soil columns	Coarse sand, Loamy sand, Clay loam and organic muck	Hepatitis A virus, Poliovirus type 1, Echovirus type 1, MS2	Few or no viruses were detected in clay loam column effluents with >99.98% virus reductions under all conditions tested. Virus reductions were greater in sandy soil columns dosed with groundwater than with wastewater.

Table 2-2. (Continued).

Author	Title	Adsorbent	Virus	Summary
Chattopadhyay and Puls (1999)	Adsorption of bacteriophages on clay minerals	Hectorite, Saponite, Kaolinite, and samples collected from a landfill site	T2, MS2, phiX174	Surface hydrophobicities of the selected sorbents and sorbates dictate sorption. Among the selected bacteriophages, maximum sorption was observed with T2 while hectorite has the maximum sorption capacity.
Syngouna and Chrysikopoulos (2010)	Interaction between viruses and clays in static and dynamic batch systems	Kaolinite, Bentonite	MS2, phiX174	Virus adsorption was higher onto bentonite than kaolinite for both MS2 and phiX174, with the only exception of phiX174 onto kaolinite at 25 ℃.
Walshe et al (2010)	Effects of pH, ionic strength, dissolved organic matter, and flow rate on the co-transport of MS2 bacteriophages with kaolinite in gravel aquifer media	Kaolinite	MS2	Decreasing the pH or increasing the ionic strength increased virus attachment. Increasing the concentration of dissolved organic matter resulted in faster virus transport velocity.

Table 2-3. Previous studies for contaminants removal from water using pyrophyllite.

Author	Title	Contaminant	Summary
Keren and Sparks (1994)	Effect of pH and ionic strength on boron adsorption by pyrophyllite	Boron	The higher capacity of pyrophyllite, in comparison to montmorillonite, to adsorb boron at pH 9.
Scheidegger at al (1996)	Investigation of Ni sorption on pyrophyllite: An XAFS study	Nickel	The results suggest that the total coverage of surface sites is not necessary for the formation of multinuclear surface complexes and implies that the pyrophyllite surface promotes hydrolysis and multinuclear complex formation.
Scheidegger at al (1997)	The kinetics of nickel sorption on pyrophyllite as monitored by x-ray absorption fine structure(XAFS) spectroscopy	Nickel	The results suggest that the formation of multinuclear Ni complexes increasing in size with progressing reaction time.
Prasad et al (2000)	Kinetics and isotherms for aqueous lead adsorption by natural minerals	Lead	The adsorption process is found to be endothermic in the case of pyrophyllite and exothermic in the case of carbonatic rock phosphate.
Saxena et al (2001)	Adsorption of cyanide from aqueous solutions at pyrophyllite surface	Cyanide	Adsorption of cyanide on the mineral surface is pH dependent and the maximum adsorption is obtained from solutions of pH 7.0.

Table 2-3. (Continued).

Author	Title	Contaminant	Summary
Gücek et al (2005)	Adsorption and kinetic studies of cationic and anionic dyes on pyrophyllite from aqueous solutions	Dyes	The results revealed that pyrophyllite can be used as low-cost adsorbents for removing both cationic and anionic dyes.
Morrow et al (2005)	Macro- and nanoscale observations of adhesive behavior for several *E. coli* strains (O157:H7 and environmental isolate) on mineral surface	*E. coli*	The results suggested that a composite form of pyrophyllite, mica, and silica appeared the strong adhesive behavior to *E.coli* attributed to the hydrophobic pyrophyllite component of the mineral.
Prasad and Saxena (2008)	Attenuation of divalent toxic metal ions using natural sericitic pyrophyllite	Divalent metal ions	The adsorption process was found to be endothermic and the Freundlich adsorption model represented the data at different temperatures more suitably.
Gupta et al (2009)	Modeling the adsorption kinetics of divalent metal ions onto pyrophyllite using the integral method	Divalent metal ions	The adsorption system was modeled and simulated to predict kinetic parameters for the adsorption of metal cations onto pyrophyllite, a low-cost adsorbent.
Sheng et al (2009)	Adsorption of methylene blue from aqueous solution on pyrophyllite	Dye	The results indicated that the ability of pyrophyllite to adsorb methylene blue increased by acid activation and milling.

III. Materials and Methods

1. Preparation and characterization of pyrophyllite

Pyrophyllite used in this study was obtained from the Sungsan Mining (Haenam, Korea). Mechanical sieving was conducted with US Standard Sieves No. 100. Pyrophyllite fractions with a grain size of less than 0.15 mm were used unless stated otherwise. Field emission scanning electron microscopy (FESEM) and Energy Dispersive X-ray Spectrometer (EDS) analyses were performed using a field emission scanning electron microscope (Supra 55VP, Carl Zeiss, Germany). The chemical composition of pyrophyllite was investigated using an X-ray fluorescence spectrometer (XRF, S4 pioneer, Bruker, Germany). The mineralogical and crystalline structural properties were examined using X-ray diffractometry (XRD, D8 Advance, Bruker, Germany) with a CuKα radiation of 1.5406Å at a scanning speed of 0.6°/sec. Infrared spectra were recorded on a Bomem MB-104 (Abb-Bomem Inc, Quebec, Canada) Fourier transform infrared (FTIR) spectrometer using KBr pellets. Surface area was determined by Brunauer-Emmett-Teller (BET) N_2 adsorption analysis using an ASAP 2010 instrument (Micromeritics, USA). The zeta potentials were measured at various pH values, which were obtained using dilute HNO_3 and NH_4OH. The point of zero charge (pH_{pzc}) of pyrophyllite was determined from the zeta potentials.

2. Virus and plaque assay

The bacteriophage MS2 (ATCC 15597-B1) was obtained from the American Type Culture Collection and was grown on *Escherichia coli* (ATCC 15597) using the double agar overlay method (Adams, 1959). MS2 is an icosahedral single-stranded RNA phage (VanDuin, 1988). Enumeration of bacteriophages was performed by the plaque assay method (Adams, 1959) using the aforementioned *E. coli* host. The host culture (0.2 mL) and 0.1 mL of the diluted virus sample was mixed with 5 mL of soft agar in a tube, and the mixture was then poured onto a trypticase soy agar (TSA) plate to solidify. After solidifying, the plates were incubated at 37 ℃ for 18h.

3. Batch experiments

3.1. Fluoride removal experiments

All chemicals used for the experiments were purchased from Sigma Aldrich. The desired fluoride solution was prepared by diluting the stocking fluoride solution (1000 mg/L; Figure 3-1), which was made from sodium fluoride (NaF). All batch experiments were performed at a solution pH of 5.5 unless stated otherwise. Equilibrium batch experiments were conducted with four different particle sizes of pyrophyllite. One gram of pyrophyllite was added to 30 mL fluoride solution (initial concentration = 4–96 mg/L) in 50 mL polypropylene conical tubes. The tubes were shaken at 25 ℃ and 40 rpm using a culture tube rotator (MG-250D72, Mega Science, Korea; Figure 3-2). The samples were collected 24 h post-reaction, and filtered through a 0.45-μm membrane filter. The fluoride concentration was measured using fluoride ion selective electrode (9609BNWP, Thermo Scientific, USA; Figure 3-3). In the fluoride measurement, total ionic strength adjustment buffer solution (58 g NaCl, 57 mL CH_3COOH, 150 mL 6M NaOH in 1000 mL deionized water) was used to prevent the interference of other ions.

Figure 3-1. Fluoride stock solution.

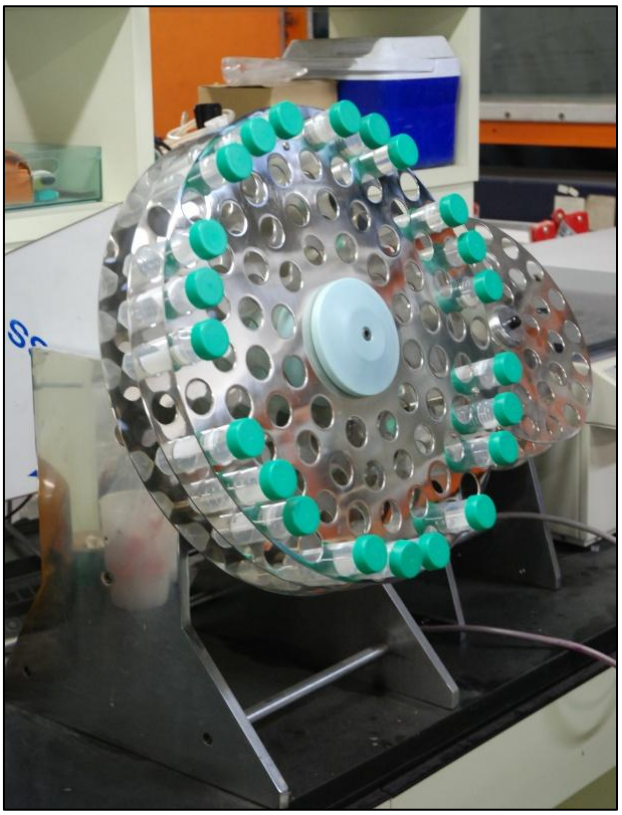

Figure 3-2. Tube rotator.

Figure 3-3. Fluoride ion selective electrode.

Next, kinetic batch experiments were performed at the initial fluoride concentration of 10 mg/L and pyrophyllite dose of 1 g. In the experiments, the samples were taken at 1, 2, 3, 6, 9, 12, 24, 36 and 48 h post-reaction. Thermodynamic experiments were conducted at 25, 35, and 45 ℃ to observe the effect of temperature on fluoride removal. The experiments were performed at the initial fluoride concentration of 10 mg/L and pyrophyllite dose of 1 g, and the samples were taken at 1, 2, 3, 6, 9, 12, 24, 36 and 48 h post-reaction. Further batch experiments were carried out to examine the effect of pyrophyllite dosage on fluoride removal. The experiments were conducted at an initial fluoride concentration of 10 mg/L with pyrophyllite dosages ranging from 0.05 to 2.0 g in 30 mL solution. The samples were collected 24 h post-reaction.

In the pH experiments, 0.1 M NaOH and 0.1 M HCl solutions were used for adjusting the pH from 2.9 to 11.0. The pH was measured with a pH probe (9107BN, Thermo Scientific, USA). In the competing anion experiments, the competing anions (Cl^-, NO_3^-, SO_4^{2-}, HPO_4^{2-}, CO_3^{2-}) were added to fluoride solution to achieve the desired anion concentrations (0.5, 1 mM). Lastly, batch experiments were performed to examine the effect of thermal treatment of pyrophyllite on fluoride removal (initial fluoride concentration = 10 mg/L; pyrophyllite dose = 0.6 g). Pyrophyllite was thermally treated at different temperature for 3 h in a programmable tube furnace (WiseTherm(R) FT-1230, DAIHAN Scientific, Korea; Figure 3-4). All experiments were performed in triplicate.

Figure 3-4. Programmable tube furnace.

3.2. Virus removal experiments

Batch experiments were also conducted in triplicate to examine the removal of bacteriophage MS2 (Figure 3-5) on pyrophyllite. MS2 stock solution was diluted from a concentrated titer with artificial ground water (AGW) to the desired concentration. The AGW included 0.075 mM $CaCl_2$, 0.082 mM $MgCl_2$, 0.051 mM KCl, and 1.5 mM $NaHCO_3$ at pH 7.6. The virus stock concentration was 10^5–10^6 plaque forming unit (pfu)/mL. The batch experiment method consisted of adding 30 mL of virus stock solution to 50 mL centrifuge tubes containing different masses of pyrophyllite (0.01–1.0 g). Pyrophyllite particles smaller than 0.15 mm (US Standard Sieves No. 100) in diameter were used. After all tubes were properly prepared and sealed, they were shaken at 40 rpm for 5 h at 4 ℃ (Figure 3-6) to avoid thermal inactivation of the virus. Suspensions were then centrifuged at 9000 x g and 4 ℃ for 15 min (Combi-514R; Hanil Science Industrial, Incheon, Korea). For further batch experiments, tubes were shaken for a set of desired reaction times ranging from 5 to 300 min (pyrophyllite = 1 g; solution volume = 30 mL). The viable bacteriophage concentration was determined by the plaque assay method. Control tubes were filled with only bacteriophage solution and treated in the same manner as the experimental tubes. The bacteriophage removal was calculated with the following formula:

$$S = \frac{C_i - C}{M} \quad (1)$$

where S is the amount of bacteriophage removed per one gram of pyrophyllite, C_i

and C are the initial and final bacteriophage concentrations in the liquid phase, respectively, and M is the total mass of pyrophyllite used in the experiment.

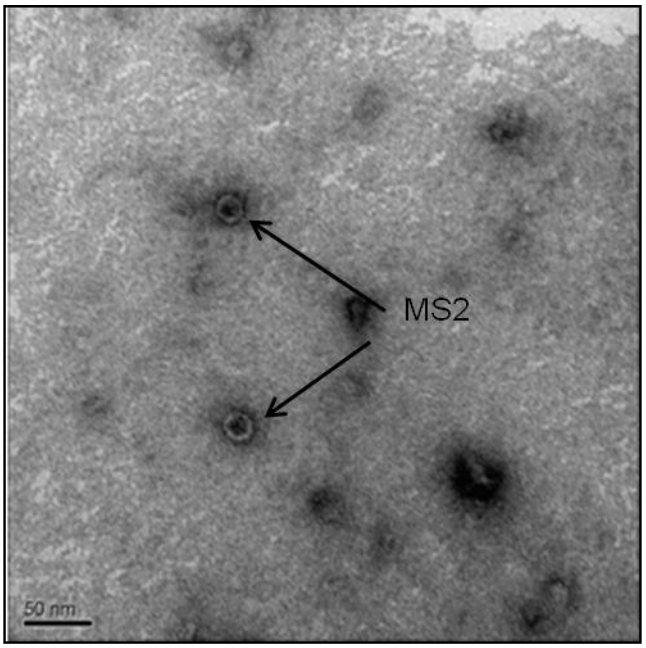

Figure 3-5. Transmission electron microscope image of bacteriophages MS2 (bar = 50 nm).

Figure 3-6. Shaking incubator.

3.3. MS2 removal in the presence of fluoride

To examine the effect of fluoride ions on bacteriophage removal, inactivation experiments for MS2 were conducted in fluoride solution in the absence of pyrophyllite. Virus stock solution containing 1.02×10^6 pfu/mL was added to a 50 mL centrifuge tube containing two different concentrations of fluoride (5 and 10 mg /L) in a 30 mL solution. The tubes were shaken at 40 rpm for 5 h at 4 ℃ to avoid thermal inactivation of the virus. In addition, batch experiments in the presence of pyrophyllite (0.1–1.0 g in 30 mL solution) were performed for MS2 removal from fluoride solution (5, 10 mg/L). In these experiments, MS2 stock solution was diluted with AGW to the desired concentration. The log removal of bacteriophage in the experiment was calculated as follows:

$$\log\ removal = -log\left(1 - \frac{R}{100}\right) \quad (2)$$

where R is the percent removal of bacteriophage during the experiment.

Pyrophyllite particles used in the column experiments were in the size range of 0.42–0.60 mm (US Standard Sieves No. 30 and No. 40) and had a particle density of 2.626 g/cm. Column experiments were performed using a Plexiglas column (inner diameter = 2.5 cm, column length = 10 cm) packed with pyrophyllite. For each column experiment, a column was packed with pyrophyllite (mass of filter materials = 70.4 ± 0.4 g) by the tap-fill method to attain a bulk density of 1.442 ± 0.012 g/cm and a porosity of 0.452 ± 0.004. Column experiments were conducted at

4 ℃ to minimize the inactivation of bacteriophage MS2. The column was connected to a pump (QG400, FASCO, USA) operating at a rate of 0.5 mL/min. Prior to an experiment, the packed column was flushed upward with 20 bed volumes (1 bed volume = 26.8 cm^3) of AGW until the column effluent was clear and a steady-state flow condition was established. Column experiments were performed in a downward flow mode with continuous injection of bacteriophage and/or fluoride in AGW at a flow rate of 0.5 mL/min. Effluent samples were collected at regular intervals for 24 h using an auto collector (Retriever 500, TELEDYNE, USA). Effluent samples were analyzed to determine the bacteriophage concentration using the double agar overlay method. The fluoride concentration was measured using a fluoride ion selective electrode (9609BNWP, Thermo Scientific, USA). In the fluoride measurement, a total ionic strength adjustment buffer solution (58 g of NaCl, 57 mL of CH_3COOH, 150 mL of 6M NaOH in 1000 mL deionized water) was used to prevent interference by other ions.

4. Data analysis

The equilibrium data can be analyzed using the following nonlinear and linear forms of Langmuir and Freundlich isotherm models:

$$q_e = \frac{Q_m K_L C_e}{1 + K_L C_e} \tag{3}$$

$$\frac{C_e}{q_e} = \frac{1}{Q_m b} + \frac{C_e}{Q_m} \tag{4}$$

$$q_e = K_F C_e^n \tag{5}$$

$$\log q_e = \log K_F + n \log C_e \tag{6}$$

where q_e is the amount of fluoride removed at equilibrium (mg/g), Q_m is the maximum mass of fluoride removed per unit mass of pyrophyllite (removal capacity), K_L is the Langmuir constant related to the binding energy, C_e is the concentration of fluoride in the aqueous solution at equilibrium, K_F is the distribution coefficient, and n is the Freundlich constant. Values of K_L, Q_m, K_F, and n can be determined by fitting the Langmuir and Freundlich models to the observed data.

The kinetic data can be analyzed using the following nonlinear and linear forms of pseudo first-order and pseudo second-order models (Ho and Mckay, 1999; Mathialagan and Viraraghavan, 2003):

$$q_t = q_e[1 - exp(-k_1 t)] \tag{7}$$

$$\log (q_e - q_t) = \log q_e - \frac{k_1}{2.303} t \quad (8)$$

$$q_t = \frac{k_2 q_e^2 t}{1 + k_2 q_e t} \quad (9)$$

$$\frac{t}{q_t} = \frac{1}{k_2 q_e^2} + \frac{t}{q_e} \quad (10)$$

where q_t is the amount of fluoride removed at time t, k_1 is the pseudo first-order rate constant, and k_2 is the pseudo second-order velocity constant.

The thermodynamic data can be analyzed using the following equations (Goswami and Purkait, 2011):

$$\log\left(\frac{aq_e}{C_e}\right) = \frac{\Delta S^\circ}{2.303R} + \frac{-\Delta H^\circ}{2.303RT} \quad (11)$$

$$\Delta G^\circ = \Delta H^\circ - T\Delta S^\circ \quad (12)$$

where a is the adsorbent dose, ΔS^0 is the change in entropy, R is the gas constant (= 8.314 J/mol/K), ΔH^0 is the change in enthalpy, T is the absolute temperature, and ΔG^0 is the change in Gibb's free energy. Values of ΔS^0 and ΔH^0 can be determined by plotting log (aq_e/C_e) versus 1/T using Equation (11), and then value of ΔG^0 can be quantified from Equation (12).

In the column experiments, the empty bed contact time (EBCT) can be determined using the following equation:

$$\text{EBCT} = \frac{V_r}{Q} \quad (13)$$

where V_r is the fixed-bed volume and Q is the volumetric flow rate. The column capacity for bacteriophage (or fluoride) removal at a given flow rate and influent concentration (C_{cap}) can be quantified using the following equation:

$$C_{cap} = \frac{Q}{1000} \int_{t=0}^{t=t_{total}} (C_0 - C)\ dt \tag{14}$$

where C_0 and C are the influent and effluent concentrations, respectively, of bacteriophage (or fluoride). The mass of bacteriophage (or fluoride) removed per unit mass of pyrophyllite in the column (removal capacity of pyrophyllite, q_a) can be determined using the following equation:

$$q_a = \frac{C_{cap}}{M_f} \tag{15}$$

where M_f is the mass of pyrophyllite in the column.

IV. Results and Discussion

1. Characteristics of pyrophyllite

The images of pyrophyllite used in the experiments are presented in Figure 4-1. The digital image showed that pyrophyllite particles are white. The FESEM images (Figure 4-2) indicated that the surface appeared to be rough and heterogeneous in surface topography. The chemical composition from XRF analysis (Table 4-1) showed that the major constituents of pyrophyllite were Si (74.03%) and Al (21.20%). The EDS patterns (Figure 4-3) demonstrated that silicon (Si) was evident at the peak position of 1.74 keV as K alpha X-ray signal. Aluminum (Al) was also detected at the peak position of 1.48 keV as K alpha X-ray signal. The XRD pattern (Figure 4-4) indicated peaks for quartz (SiO_2), dickite ($Al_2Si_2O_5(OH)_4$), and pyrophyllite ($Al_2Si_4O_{10}(OH)_2$). In the FT-IR spectra (Figure 4-5), a band recorded at 3652 (1/cm) corresponded to O-H stretching vibrations for OH groups bonded to Al ions. A band at 938 (1/cm) was attributed to OH bending vibrations for Al-OH groups. N_2 adsorption-desorption analysis indicated that BET surface area of pyrophyllite was 1.3419 m^2/g with total pore volume of 5.74×10^{-4} cm^3/g and average pore diameter of 1.7122 nm (Table 4-2).

Figure 4-1. Pyrophyllite used in the experiments.

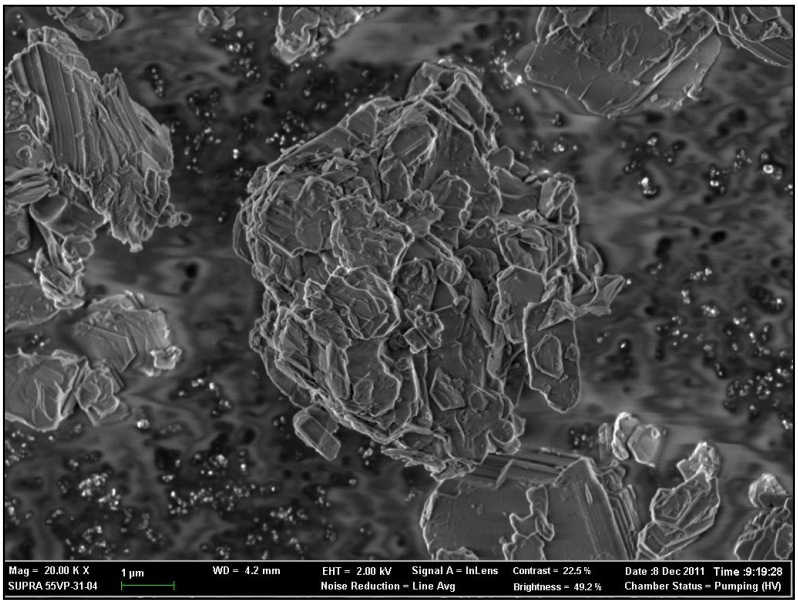

Figure 4-2. Field emission scanning electron microscope (FESEM) image of pyrophyllite (bar = 1 μm).

Table 4-1. Chemical compositions of pyrophyllite used in the experiments (data from X-ray fluorescence (XRF) analysis).

Chemical compositions (weight %)					
SiO_2	Al_2O_3	SO_3	Fe_2O_3	Others	Total
74.03	21.20	2.387	1.885	0.498	100

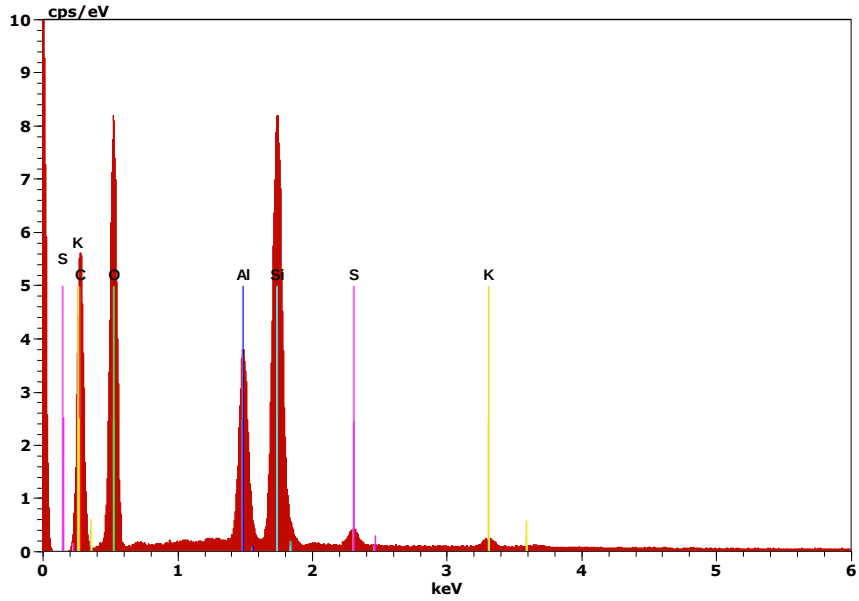

Figure 4-3. Energy dispersive X-ray spectrometer (EDS) pattern of pyrophyllite.

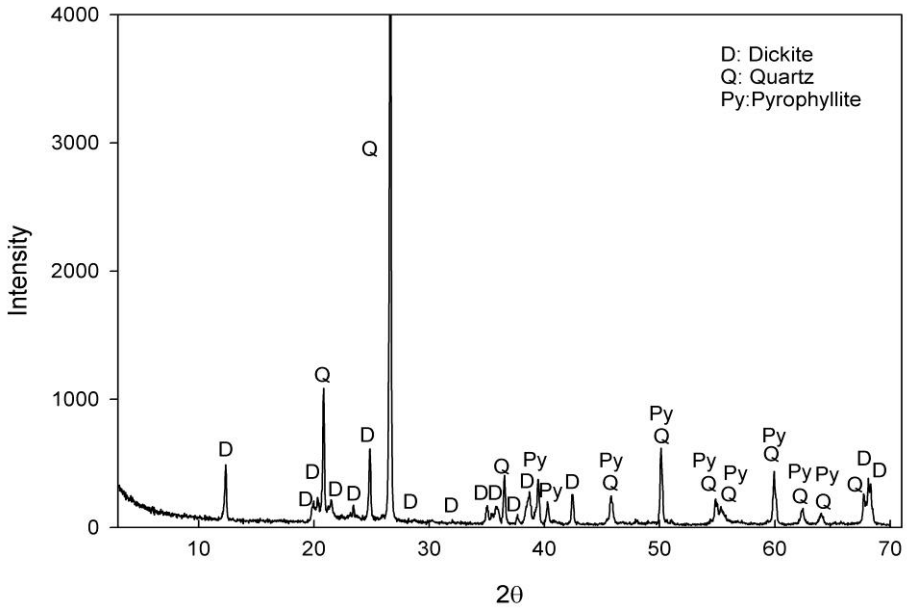

Figure 4-4. X-ray diffraction (XRD) pattern of pyrophyllite.

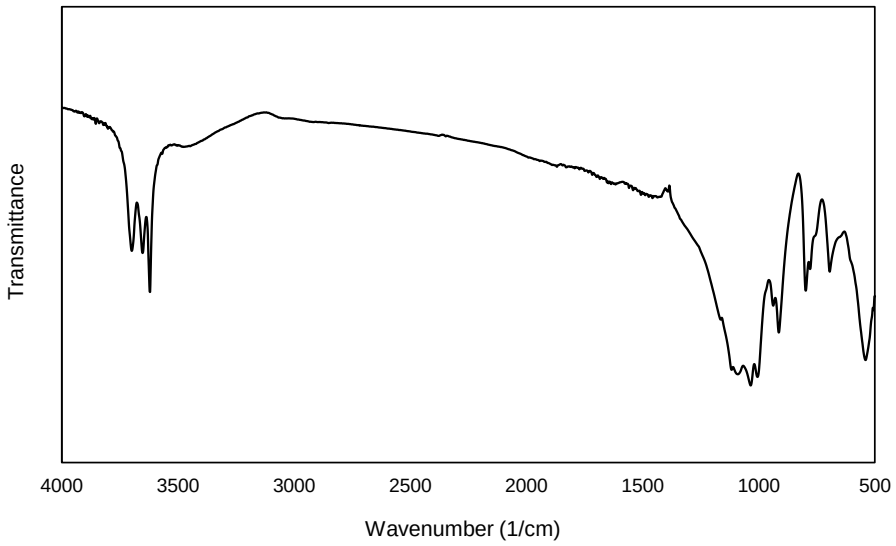

Figure 4-5. Fourier transformed infrared (FTIR) spectra of pyrophyllite.

Table 4-2. BET surface area, total pore volume, and average pore diameter of pyrophyllite (data from N_2 adsorption-desorption isotherm analysis).

BET surface area (m^2/g)	Total pore volume (cm^3/g)	Average pore diameter (nm)
1.3419	5.74×10^{-4}	1.7122

2. Fluoride removal by pyrophyllite

The equilibrium isotherms of fluoride on pyrophyllite with different particle sizes are presented in Figure 4-6. The equilibrium isotherm constants are summarized in Table 4-3. In the Freundlich model, the distribution coefficient (K_F) was in the range from 0.174 to 0.247 L/g, while the Freundlich constant (n) was between 0.224 and 0.250. In the Langmuir model, the Langmuir constant (K_L) was in the range from 0.246 to 0.310 L/mg, while the removal capacity (Q_m) was between 0.488 and 0.649 mg/g. The correlation coefficient (R^2) of the Freundlich model was greater than that of the Langmuir model, indicating that the Freundlich isotherm was appropriate at describing the experimental result. Among the particles tested, the one with particle size of < 0.15 mm showed the highest adsorption capacity of 0.737 mg/g, which was in the ranges of the removal capacity for clays/modified clays (0.045–4.24 mg/g) reported in the literature (Bhatnagar et al., 2011).

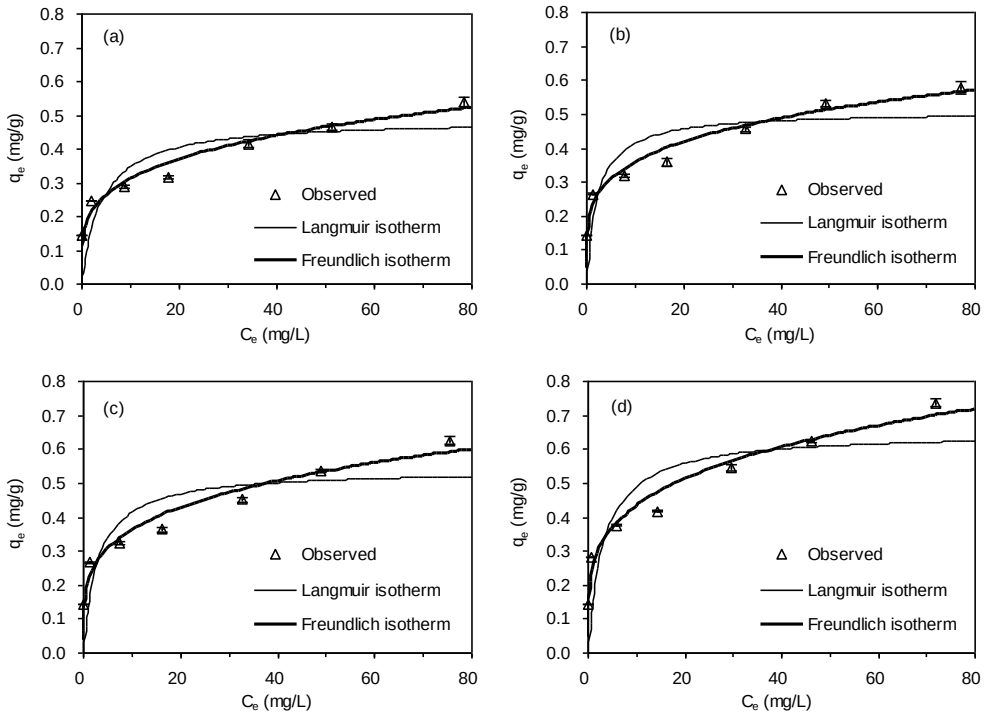

Figure 4-6. Equilibrium batch data and model fit for fluoride adsorption to pyrophyllite with different particle sizes (mm): (a) 0.42–0.85; (b) 0.25–0.42; (c) 0.15–0.25; (d) < 0.15.

Table 4-3. Equilibrium isotherm constants for fluoride adsorption by pyrophyllite with different particle sizes.

Particle size (mm)	Freundlich isotherm model			Langmuir isotherm model		
	K_F (L/g)	n	R^2	K_L (L/mg)	Q_m (mg/g)	R^2
0.42–0.85	0.174	0.250	0.942	0.246	0.488	0.653
0.25–0.42	0.213	0.224	0.943	0.440	0.508	0.646
0.15–0.25	0.204	0.246	0.928	0.333	0.539	0.640
< 0.15	0.247	0.244	0.948	0.310	0.649	0.701

The sorption kinetics of fluoride in pyrophyllite (size < 0.15 mm; initial fluoride concentration = 10 mg/L) is shown in Figure 4-7. The sorption reached equilibrium around 24 h of reaction time. Model parameters for the pseudo first-order and pseudo second-order models obtained from the kinetic experiments are provided in Table 4-4. In the pseudo first-order model, the value of q_e was 0.263 mg/g while the value of k_1 was 0.244 1/h. The value of q_e from the pseudo second-order model was greater than that from the pseudo first-order model. The value of q_e was 0.297 mg/g, while the values of k_2 was 1.023 g/mg/h. The correlation coefficients (R^2) indicated that the pseudo first-order model described the kinetic data better than the pseudo second-order model. The adsorption of fluorine ions (F^-) to pyrophyllite surfaces could be described by ligand exchange mechanism. In the adsorption process, fluorine ions could replace hydroxyl ions (OH^-) on the surfaces of pyrophyllite (Al-OH $\rightarrow$ Al-F). Additionally, below pH_{pzc} where pyrophyllite is positively charged, electrostatic attraction could occur between negatively-charged fluorine ions and positively-charged surfaces of pyrophyllite ($Al\text{-}OH_2^+ \leftrightarrow F^-$) (Ayoob et al., 2008). Note that the pH_{pzc} of pyrophyllite was determined to be 9.2.

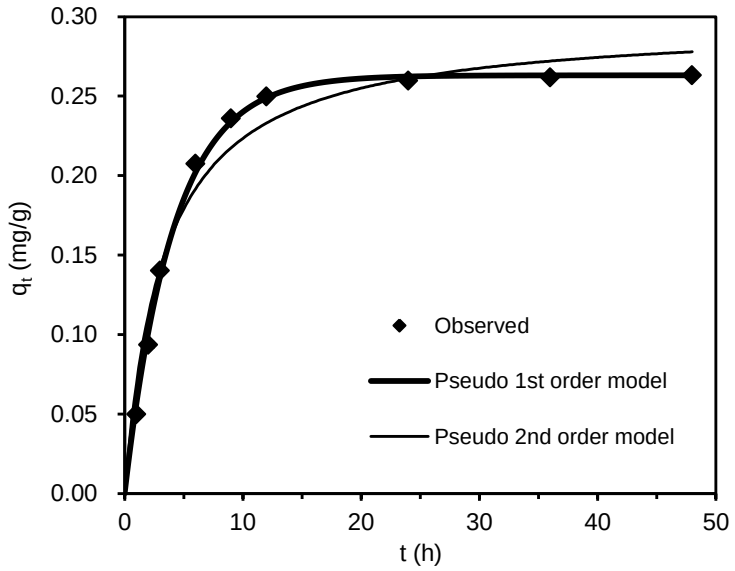

Figure 4-7. Kinetic batch data and model fit for fluoride adsorption to pyrophyllite (particle size < 0.15 mm; initial fluoride concentration = 10 mg/L).

Table 4-4. Kinetic model parameters obtained from model fitting to experimental data.

Pseudo first-order model			Pseudo second-order model		
q_e (mg/g)	k_1 (1/h)	R^2	q_e (mg/g)	k_2 (g/mg/h)	R^2
0.263	0.244	0.998	0.297	1.023	0.978

The thermodynamic data and analysis for fluoride sorption to pyrophyllite is presented in Figure 4-8. Thermodynamic parameters are provided in Table 4-5. Fluoride adsorption to pyrophyllite increased with increasing temperature from 25 to 45 ^{o}C, demonstrating that the sorption process was endothermic. The positive value of $\Delta H°$ also indicated the endothermic nature of fluoride sorption. The positive value of $\Delta S°$ showed that the randomness increased at the interface between solid and solution during the sorption process. The negative value of $\Delta G°$ indicated that the sorption process was spontaneous. This result confirms well with the reports of other researchers who examined the endothermic nature of fluoride adsorption to clay particles such as Mg/Al/Fe layer double hydroxides (Ma et al., 2011), magnesium incorporated bentonite (Thakre et al., 2010), attapulgite (Zhang et al., 2009), and micronized kaolinite (Meenakshi et al., 2008). However, Goswami and Purkait (2011) who examined the effect of temperatures on fluoride sorption to pyrophyllite reported that the sorption was exothermic, decreasing with increasing temperature from 24 to 60 ^{o}C.

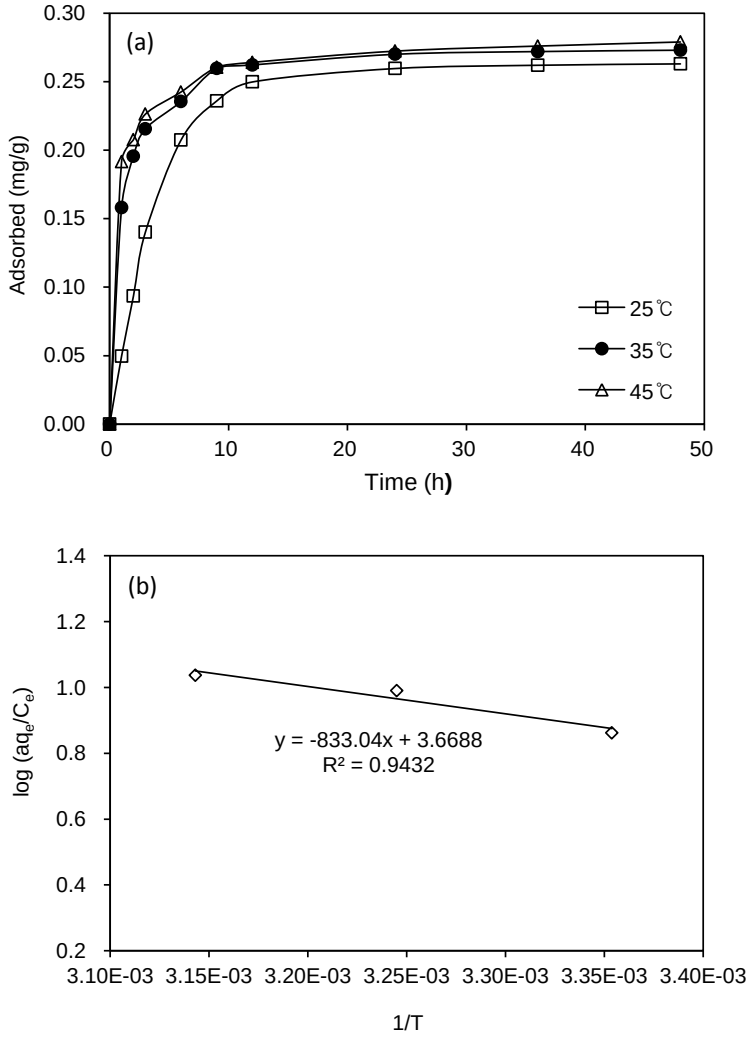

Figure 4-8. Thermodynamic data and analysis for fluoride adsorption to pyrophyllite (particle size < 0.15 mm; initial fluoride concentration = 10 mg/L): (a) effect of temperature on fluoride sorption; (b) determination of thermodynamic parameter.

Table 4-5. Thermodynamic parameters for fluoride adsorption to pyrophyllite.

Temperature (℃)	ΔH° (kJ/mol)	ΔS° (J/K mol)	ΔG° (kJ/mol)
25	15.95	70.25	-4.99
35			-5.70
45			-6.40

The effect of pyrophyllite dose on fluoride sorption in pyrophyllite (particle size < 0.15 mm; initial fluoride concentration = 10 mg/L) is presented in Figure 4-9. The removal percent increased from 25.0 to 98.5% with increasing pyrophyllite doses from 0.05 to 2.0 g/L. Meanwhile, adsorption capacity decreased from 1.414 to 0.139 mg/g with increasing pyrophyllite doses. Results indicated that initial fluoride concentration of 10 mg/L could be reduced to < 1.5 mg/L at pyrophyllite dose ≥ 1.0 g/L.

The effect of solution pH on fluoride removal in pyrophyllite (particle size < 0.15 mm; initial fluoride concentration = 10 mg/L) is shown in Figure 4-10. The adsorption capacity at pH 4.0 was 0.278 mg/g and decreased slightly to 0.276 mg/g at pH 5.9. As the solution pH further increased and approached 9.0, the adsorption capacity decreased slightly to 0.260 mg/g, indicating that fluoride removal in pyrophyllite was not sensitive to solution pH changes between 4.0 and 9.0 under given experimental conditions. However, the adsorption capacity decreased considerably to 0.146 mg/g at pH 2.9. In highly acidic pH, fluoride could exist preferably as the form of HF, and so the adsorption of fluoride to pyrophyllite could be reduced greatly. At pH 11.0, the adsorption capacity decreased sharply to 0.004 mg/g. In highly alkaline pH, fluoride could exist preferably as NaF form due to addition of NaOH into solution, which results in the sharp decrease of fluoride adsorption to pyrophyllite. Our results conform well with the report of Goswami and Purkait (2011) who investigated the adsorption of fluoride to pyrophyllite.

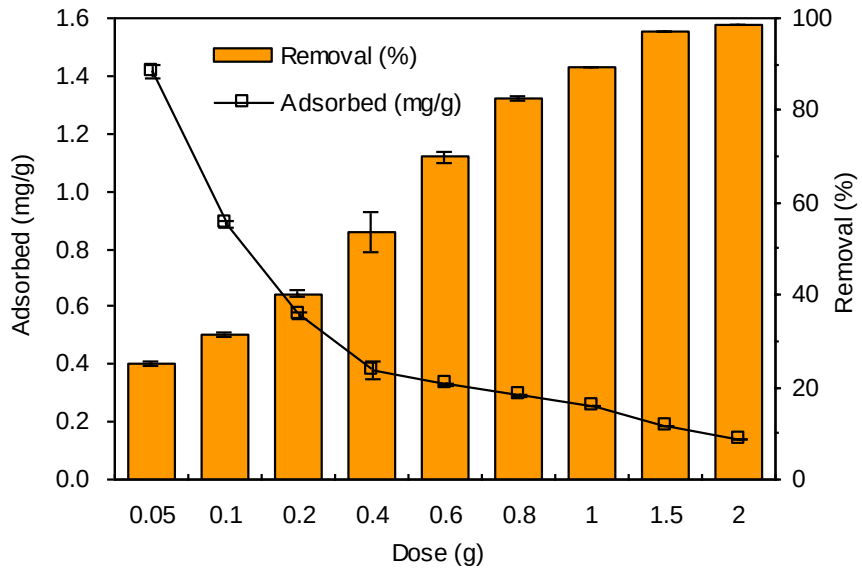

Figure 4-9. Effect of pyrophyllite dose on fluoride adsorption (particle size < 0.15 mm; initial fluoride concentration = 10 mg/L).

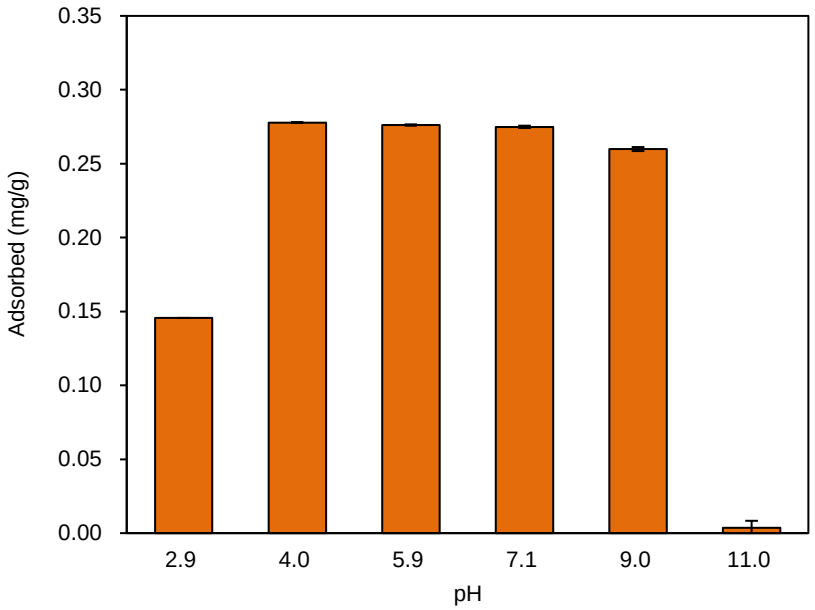

Figure 4-10. Effect of solution pH on fluoride adsorption to pyrophyllite (particle size < 0.15 mm; initial fluoride concentration = 10 mg/L).

The effect of anions on the removal of fluoride in pyrophyllite (particle size < 0.15 mm; initial fluoride concentration = 10 mg/L) is presented in Figure 4-11. Chloride (Cl^-) and nitrate (NO_3^-), monovalent anions, showed minimal effect on the removal of fluoride in pyrophyllite at concentrations ranging from 0.5 to 1 mM. This result agreed well with the previous reports (Karthikeyan et al., 2005; Meenakshi et al., 2008), showing that the effects of Cl^- and NO_3^- on fluoride removal in clay adsorbents was negligible. Meanwhile, divalent anions such as sulfate (SO_4^{2-}), phosphate (HPO_4^{2-}), and bicarbonate (CO_3^{2-}) profoundly interfered with the removal of fluoride in pyrophyllite. Goswami and Purkait (2011) reported that the adsorption of fluoride to pyrophyllite decreased slightly from 84 to 79% with increasing sulfate ions from 3.1 to 12.5 mg/L. Divalent anions are known to have a higher affinity to adsorbents than monovalent anions. Our results indicated that the removal of fluoride in pyrophyllite was most affected by CO_3^{2-}. At the given experimental conditions, the impact of the divalent anions was in the order of $SO_4^{2-} < HPO_4^{2-} < CO_3^{2-}$.

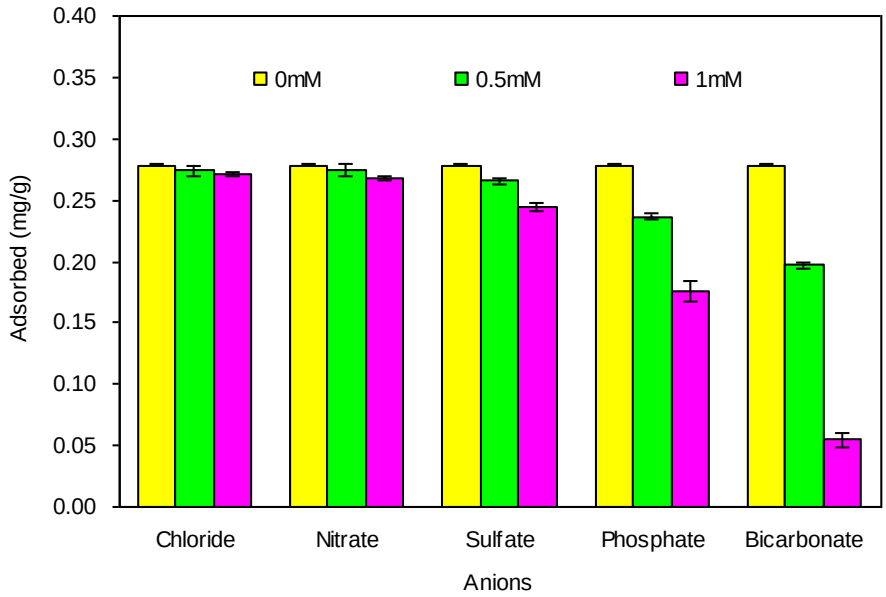

Figure 4-11. Effect of anions on fluoride adsorption to pyrophyllite (particle size < 0.15 mm; initial fluoride concentration = 10 mg/L).

The adsorption capacities for fluoride removal by pyrophyllite thermally treated under different temperatures are provided in Figure 4-12. Thermal treatment influenced the adsorption capacity of pyrophyllite. In given experimental conditions (adsorbent dosage = 0.6 g; fluoride concentration = 10 mg/L; solution volume = 30 mL), the adsorption capacity (= 0.399 mg/g) was the highest in the adsorbent treated at 400 ^{o}C (A-400), which is 21% higher than that (= 0.329 mg/g) of untreated pyrophyllite (UT). At higher temperatures (600, 800 ^{o}C), the adsorption capacities of A-600 and A-800 sharply decreased to ~0.10 mg/g. At 1000 and 1100 ^{o}C, the adsorption capacities of A-1000 and A-1100 decreased further to ~0.02 mg/g.

This result could be attributed to the fact that thermal treatment could alter the mineralogical and physical properties of pyrophyllite. XRD patterns of pyrophyllite treated under different temperatures are presented in Figure 4-13. Also, the mineralogical property and BET surface area of thermally treated pyrophyllite are provided in Table 4-6. Untreated pyrophyllite (UT) showed the general XRD pattern found in the literature (Bentayeb et al., 2003), possessing the peaks of quartz (SiO_2, hexagonal), dickite ($Al_2Si_2O_5(OH)_4$), and pyrophyllite ($Al_2Si_4O_{10}(OH)_2$). A-400 had the same XRD pattern as UT with the peaks of quartz, dickite, and pyrophyllite. In addition, A-400 had the surface area of 1.673 m^2/g, which is about 24% higher than that (=1.342 m^2/g) of UT. Above 600 ^{o}C, however, the general XRD pattern of pyrophyllite was disappeared. A-600 and A-800 had the peaks of quartz with the surface areas of 1.935 and 1.475 m^2/g, respectively. At 1000 and 1100 ^{o}C, the peaks of mulite ($Al_6Si_2O_{13}$) and cristobalite (SiO_2, tetragonal) were

appeared along with the quartz peaks. A-1000 and A-1100 had the surface areas of 0.992 and 0.420 m^2/g, respectively.

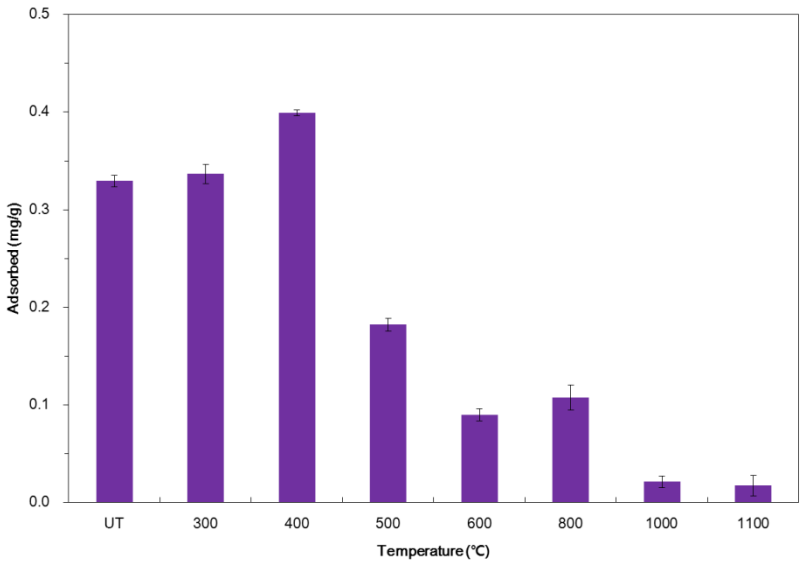

Figure 4-12. Effect of thermal treatment of pyrophyllite on fluoride adsorption (UT = untreated; particle size < 0.15 mm; initial fluoride concentration = 10 mg/L).

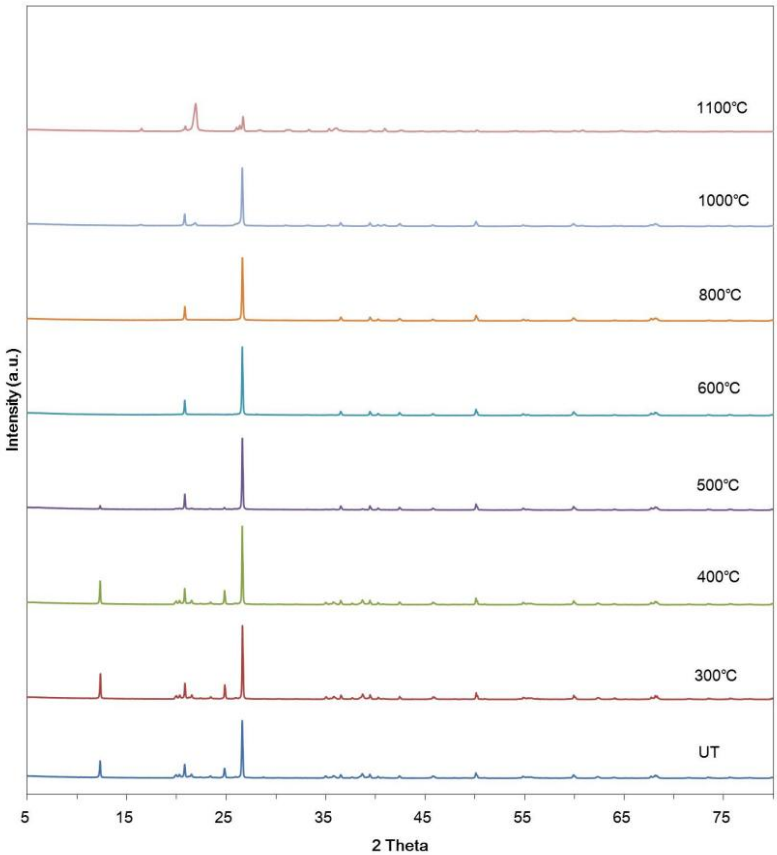

Figure 4-13. X-ray diffraction patterns of pyrophyllite thermally treated at different temperatures (UT = untreated).

Table 4-6. Characteristics of pyrophyllite thermally treated at different temperatures.

Temperature (^{o}C)	UT	300	400	500	600	800	1000	1100
BET surface area (m^2/g)	1.342	1.315	1.673	1.650	1.935	1.475	0.992	0.420
Properties (XRD peak)	Q, D, Py	Q, D, Py	Q, D, Py	Q, D, Py	Q	Q	Q, C, M	Q, C, M

UT: untreated; Q: quartz; D: dickite; Py: pyrophyllite; C: cristobalite; M: mulite

3. Bacteriophage MS2 removal by pyrophyllite

Figure 4-14 shows the removal of bacteriophage MS2 on pyrophyllite as a function of adsorbent dose (solution volume = 30 mL; initial MS2 concentration = 2.85×10^6 pfu/mL). The percent removal increased from 5.26% to 99.99% as the pyrophyllite dose increased from 0.01 to 1.0 g per 30 mL. The removal capacity of the pyrophyllite increased from 4.50×10^8 to 7.94×10^8 pfu/g as the adsorbent dose increased from 0.01 to 0.1 g per 30 mL, and then, the capacity decreased to 8.55×10^7 pfu/g as the dose increased to 1.0 g per 30 mL. More than 99% of the bacteriophage MS2 could be removed with a pyrophyllite dose $\geq$ 0.2 g per 30 mL.

Figure 4-15 shows the removal of bacteriophage MS2 on a given dose of pyrophyllite (1 g per 30 mL solution; initial MS2 concentration = 4.62×10^6 pfu/mL) as a function of reaction time. The sorption of MS2 to pyrophyllite from aqueous solution was rapid. Within 30 min, approximately 99.98% (= 3.7 log removal) of MS2 was attained. More than 4.0 log removal was achieved after 180 min with a removal capacity of 1.39×10^8 pfu/g. The literature reported that virus sorption to clay particles is generally rapid. Sobsey et al (1980) reported that the adsorption of poliovirus and reovirus on bentonite and kaolinite reached equilibrium within 15 min. Park et al (2011) showed that sorption of bacteriophage MS2 on Mg/Fe layered double hydroxide reached equilibrium within 60 min.

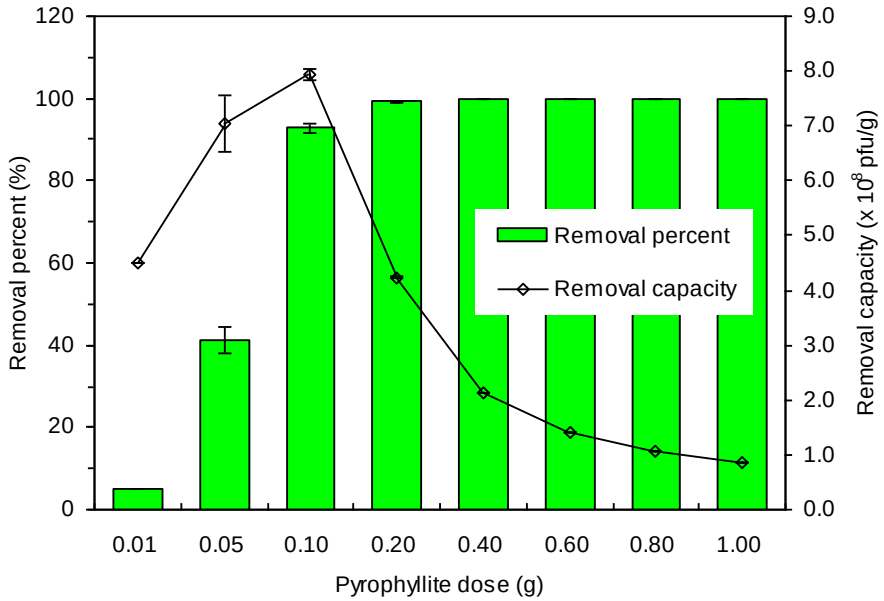

Figure 4-14. The removal of bacteriophage MS2 in pyrophyllite as a function of adsorbent dose (solution volume = 30 mL; initial MS2 concentration = 2.85×10^6 pfu/mL).

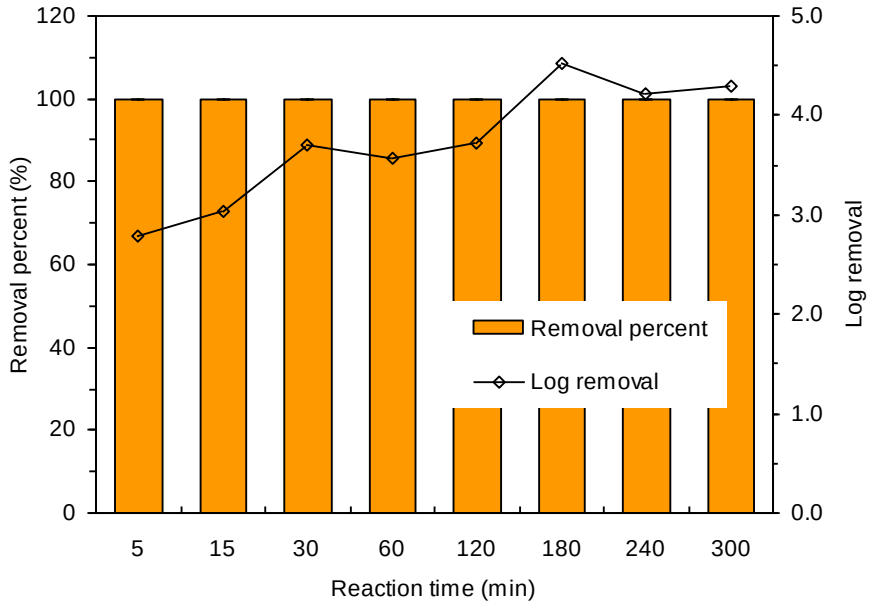

Figure 4-15. The removal of bacteriophage MS2 in pyrophyllite as a function of reaction time (1 g pyrophyllite in 30 mL solution; initial MS2 concentration = 4.62 $\times 10^6$ pfu/mL).

The Freundlich and Langmuir isotherm models were used to analyze the sorption data (Figure 4-16). The parameters for the Freundlich isotherm were determined by plotting log q_e versus log C_e (Figure 4-16a), while the parameters for the Langmuir isotherm were determined by plotting q_e/C_e versus C_e (Figure 4-16b). The Freundlich and Langmuir constants are provided in Table 4-7. The correlation coefficients showed that the Langmuir model was more suitable than the Freundlich model for bacteriophage MS2 sorption. The maximum amount of MS2 removed per unit mass of pyrophyllite (Q_m) was determined to be 5.01×10^8 pfu/g. Pyrophyllite had a relatively high adsorption capacity compared to other materials. Jin et al (2007) found that the adsorption capacities of Mg/Al and Ni/Al LDHs for MS2 and Phix174 were $1.4 \times 10^7 - 2.1 \times 10^7$ pfu/g. Park et al (2011) reported that adsorption capacity for MS2 by Mg/Fe LDH calcined at 300 ℃ was 2.34×10^8 pfu/g.

Figure 4-17 presents the pseudo first-order and pseudo second-order kinetic models that were used to analyze rate data. The parameters of the pseudo first-order model were determined by plotting log (q_e - q_t) versus t (Figure 4-17a), while the parameters of the pseudo second-order model were determined by plotting log q_t/t versus t (Figure 4-17b). The kinetic model parameters are provided in Table 4-8. The amount of MS2 removed at equilibrium (q_e) was determined to be 1.43×10^8 pfu/g, based on the pseudo second-order model. The correlation coefficient showed that pseudo second-order model was better than pseudo first-order model at describing the kinetics of sorption of MS2 on pyrophyllite.

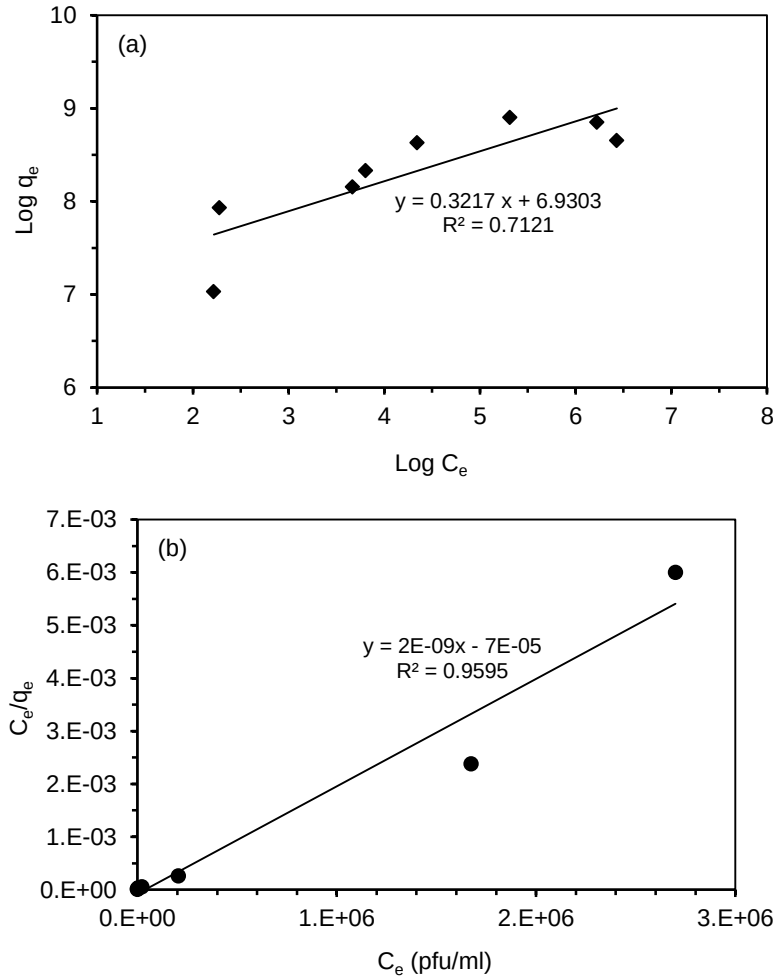

Figure 4-16. Adsorption isotherm model analysis: (a) Freundlich model; (b) Langmuir model.

Table 4-7. Equilibrium model-fitted parameters based on experimental data.

Freundlich model			Langmuir model		
K_F (L/g)	n	R^2	Q_m (pfu/g)	K_L (mL/pfu)	R^2
8.52×10^5	0.32	0.71	5.01×10^8	2.86×10^{-5}	0.96

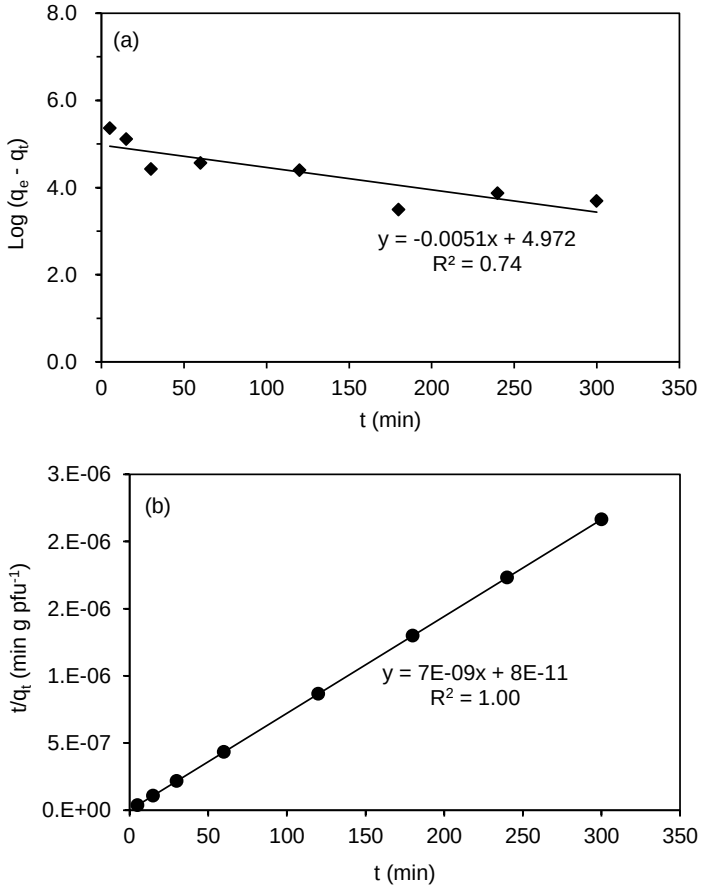

Figure 4-17. Sorption kinetic model analysis: (a) pseudo first-order model; (b) pseudo second-order model.

Table 4-8. Kinetic model-fitted parameters based on experimental data.

Pseudo first-order model			Pseudo second-order model		
q_e (pfu/g)	k_1 (1/min)	R^2	q_e (pfu/g)	k_2 (g/pfu/min)	R^2
1.39×10^{8}	1.17×10^{-2}	0.74	1.43×10^{8}	6.13×10^{-7}	1.00

4. Removal of fluoride and bacteriophage by pyrophyllite

Preliminary tests were performed to examine the effect of fluoride ions on bacteriophage MS2 inactivation. The tests were conducted with a reaction time of 5 h in the absence of pyrophyllite at initial MS2 concentrations of 1.02×10^6 pfu/mL and fluoride concentrations of 5 and 10 mg/L. No inactivation of MS2 was observed at 5 mg/L fluoride, while 19.3% of the initial MS2 was inactivated at 10 mg/L fluoride. Further tests were performed in the presence of pyrophyllite to observe the effect of fluoride ions on MS2 removal at fluoride concentrations of 5 and 10 mg/L with a reaction time of 5 h (Figure 4-18). At a pyrophyllite dose of 1.0 g per 30 mL, the log removal in the presence of 5 mg/L fluoride was 3.05, which was lower than that for 0 mg/L fluoride. At the same dose of pyrophyllite, the log removal in the presence of 10 mg/L fluoride was 2.54, which was lower than those for 0 and 5 mg/L fluoride. The removal of MS2 by pyrophyllite was thus shown to be influenced by fluoride ions. The fluoride results could be attributed to fluoride ions competing with bacteriophage MS2 for sorption sites on the pyrophyllite surface. Separate batch experiments indicated that the fluoride adsorption capacity on pyrophyllite was 0.124 mg/g at the given conditions (pyrophyllite dose = 1.0 g per 30 mL; initial fluoride concentration = 5 mg/L; reaction time = 5 h), which indicated that fluoride could adsorb on pyrophyllite. As mentioned above, the MS2 inactivation at 5 mg/L fluoride was negligible, which meant that fluoride ions could only affect MS2 removal on pyrophyllite through occupation of sorption sites and

thereby could decrease MS2 adsorption on pyrophyllite. The MS2 removal on pyrophyllite was lower at 10 mg/L fluoride than that at 5 mg/L fluoride, even though the MS2 inactivation by fluoride also contributed to MS2 removal at 10 mg/L fluoride. This indicated that MS2 adhesion to pyrophyllite was further decreased at 10 mg/L fluoride because more sorption sites on pyrophyllite were occupied by fluoride ions.

The adsorption of fluoride to pyrophyllite could be described by a ligand exchange mechanism as fluoride ions could replace hydroxyl ions on the surfaces of pyrophyllite during adsorption (Goswami and Purkait, 2011). Viruses have carboxyl (COOH) groups on their surfaces because they contain protein polypeptides, which are composed of amino acids (Gerba, 1984). Thus, bacteriophage may adhere to the surfaces of pyrophyllite via replacement of hydroxyl ions like humic acids. It was reported that humic acids have carboxyl groups on their surfaces and adsorb to metal (aluminum, iron) oxides through replacement of hydroxyl ions on the surfaces of metal oxides (Chi and Amy, 2004; Foppen et al., 2008). However, the electrostatic attraction between bacteriophage MS2 and pyrophyllite is not favorable. It is known that MS2 has an isoelectric point of 3.9 (Zerda, 1982); thus, it is negatively charged at our solution condition (AGW = pH 7.6). The zeta potential of pyrophyllite in AGW was determined to be −22.8 mV, indicating that it was also negatively charged.

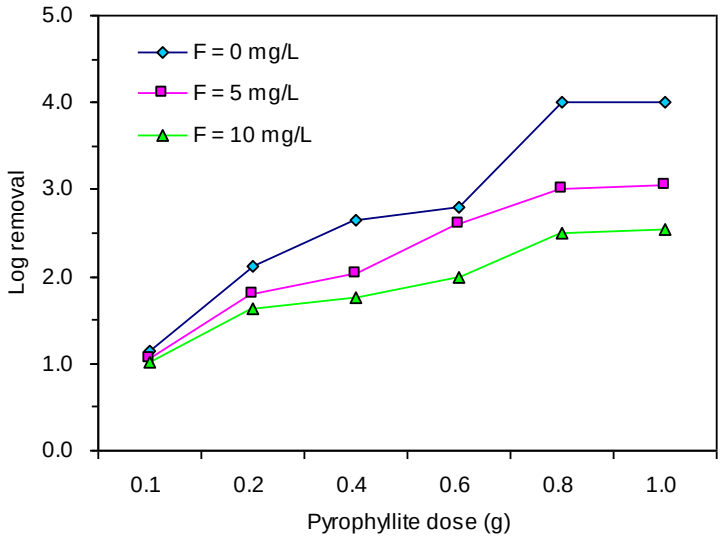

Figure 4-18. Effect of fluoride (F) on bacteriophage removal by pyrophyllite.

The breakthrough curves (BTCs) for bacteriophage MS2 and fluoride obtained from the column experiments are shown in Figure 4-19. The BTCs for MS2 are shown as bed volume versus log relative concentration, while the fluoride BTCs are presented as bed volume versus relative concentration. The BTCs show that the log relative concentration of the bacteriophage remained between −5.0 and −4.0 while the relative fluoride concentration gradually increased with increasing bed volume. The column experimental results are shown in Table 4-8. In the absence of fluoride (Ex. 1), the column capacity for bacteriophage removal (C_{cap}) was 5.74×10^8 pfu, which was slightly higher than that (= 3.33×10^8 pfu) in Ex. 2 when fluoride was present. In case of fluoride, the value of C_{cap} for fluoride in Ex. 2 was 1.61 mg, which was slightly lower than that (= 1.73 mg) in Ex. 3 when MS2 was absent. The removal capacity (q_a) for MS2 was 8.17×10^6 pfu/g in Ex. 1 and 4.70×10^6 pfu/g in Ex. 2. For fluoride, the values of q_a in Exs. 2 and 3 were 0.023 and 0.025 mg/g, respectively. The column results indicated that pyrophyllite was effective in the removal of bacteriophage under flow-through conditions. In addition, the effect of fluoride on MS2 removal in the column experiments was not as large as the fluoride effect in the batch experiments under the tested conditions. Compared to batch conditions, the contact time in flow-through conditions is short. Therefore, number of sorption sites occupied by contaminants is far smaller in column experiments than in batch experiments. In our column experiments, EBCT was 53 min, and so competition between fluoride ions and bacteriophages on the sorption sites of pyrophyllite was not significant.

Table 4-8. Experimental conditions and results for bacteriophage MS2 and fluoride removal in flow-through columns containing pyrophyllite.

Ex	MS2 concentration (pfu/mL)	Fluoride concentration (mg/L)	Flow rate (mL/min)	EBCT (min)	M_f (g)	C_{cap}		q_a	
						MS (pfu)	Fluoride (mg)	MS (pfu/g)	Fluoride (mg/g)
1	5.98×10^5	-	0.5	53.4	70.2	5.74×10^8	-	8.17×10^6	-
2	3.70×10^5	5.0	0.5	53.9	70.9	3.33×10^8	1.61	4.70×10^6	0.023
3	-	5.0	0.5	53.3	70.1	-	1.73	-	0.025

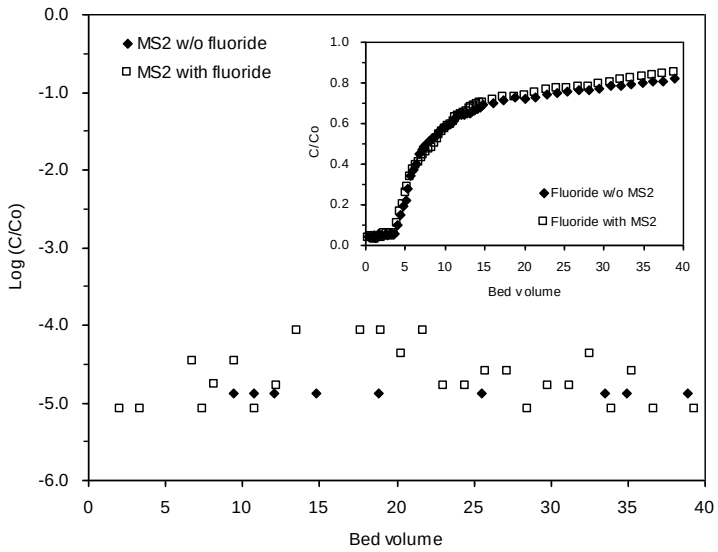

Figure 4-19. Breakthrough curves for bacteriophage MS2 and fluoride in columns containing pyrophyllite.

V. Conclusions

The removal of fluoride by pyrophyllite was examined. Results showed that pyrophyllite was effective in the removal of fluoride (maximum sorption capacity = 0.737 mg/g). Kinetic test indicated that fluoride sorption to pyrophyllite arrived at equilibrium around 24 h. Thermodynamic test indicated that fluoride sorption to pyrophyllite was endothermic. Results also demonstrated that fluoride removal was not sensitive to solution pH between 4.0 and 9.0. The influence of divalent anions (SO_4^{2-}, CO_3^{2-}, HPO_4^{2-}) on the fluoride removal was important. In addition, pyrophyllite thermally treated at 400 ^oC had the higher sorption capacity than that of untreated pyrophyllite.

Also, batch and column experiments were conducted to investigate the removal of bacteriophage MS2 from aqueous solution using pyrophyllite. Batch results demonstrated that pyrophyllite was effective at removing MS2 through the adhesion of the bacteriophage to pyrophyllite. Results also indicated that the removal of MS2 by pyrophyllite was influenced by fluoride ions. The log removal of MS2 in the presence of fluoride was lower than that when no fluoride was present. This could be attributed to fluoride ions competing with MS2 for sorption sites on the pyrophyllite surfaces. Column results showed that pyrophyllite was also effective in MS2 removal under flow-through conditions. The effect of fluoride on MS2 removal in the column experiments was not substantial compared to the effect in batch experiments. This study demonstrates the potential use of pyrophyllite for fluoride and virus removal from water.

VI. References

Adams MH.. 1959. Bacteriophages, Interscience Publishers, New York, USA.

Ayoob S, Gupta AK, Bhat VT. 2008. A conceptual overview on sustainable technologies for the defluoridation of drinking water. *Critical Reviews in Environmental Science and Technology* **38**: 401-470.

Ayoob S, Gupta AK. 2006. Fluoride in drinking water: A review on the status and stress effects. *Critical Reviews in Environmental Science and Technology* **36**: 433-487.

Bentayeb A, Amouric M, Olives J, Dekayir A, Nadiri A. 2003. XRD and HRTEM characterization of pyrophyllite from Morocco and its possible applications. *Applied Clay Science* **22**: 211–221.

Bhatnagar A, Kumar E, Sillanpää M. 2011. Fluoride removal from water by adsorption: A review. *Chemical Engineering Journal* 171: 811–840.

Bosch A, Guix S, Sano D, Pinto FM. 2008. New tools for the study and direct surveillance of viral pathogens in water. *Current Opinion in Biotechnology* **19**: 295-301.

Chattopadhyay S, Puls R. 1999. Adsorption of bacteriophages on clay minerals. *Environmental Science and Technology* 33: 3609–3614.

Chaturvedi AK, Pathak KC, Singh VN. 1988. Fluoride removal from water by adsorption on china clay. *Applied Clay Science* **3**: 337-346.

Chen H, Wang A. 2007. Kinetic and isothermal studies of lead ion adsorption onto palygorskite clay. *Journal of Colloid and Interface Science* **307**: 309-316.

Chi FH, Amy GL. 2004. Kinetic study on the sorption of dissolved natural organic matter onto different aquifer materials: the effects of hydrophobicity and functional groups. *Journal of Colloid and Interface Science* **274**: 380-391.

Foppen JWA, Lien Y, Schijven JF. 2008. Effect of humic acid on the attachment of *Eschrichia coli* in columns of goetite-coated sand. *Water Research* **42**: 211-219.

Gerba CP.. 1984. Applied and theoretical aspects of virus adsorption to surfaces.

Advances in Applied Microbiology **30**: 133-168.

Goswami A, Purkait MK. 2011. Kinetic and equilibrium study for the fluoride adsorption using pyrophyllite. *Separation Science and Technology* **46**: 1797–1807.

Gupta N, Prasad M, Singhal N, Kumar V. 2009. Modeling the adsorption kinetics of divalent metal ions onto pyrophyllite using the integral method. *Industrial and Engineering Chemistry Research* **48**: 2125–2128.

Gücek A, Sener S, Bilgen S, Mazmancı MA. 2005. Adsorption and kinetic studies of cationic and anionic dyes on pyrophyllite from aqueous solutions. *Journal of Colloid and Interface Science* **286**: 53–60.

Ho YS, Mckay G. 1999. Pseudo-second order model for sorption processes. *Process Biochemistry* **34**: 451-465.

Indian minerals yearbook 2010. 2011. Indian Bureau of Mines. 65.1–65.6.

Jin S, Fallgren PH, Morris JM, Chen Q. 2007. Removal of bacteria and viruses from waters using layered double hydroxide nanocomposites. *Science and Technology of Advanced Materials* **8**: 67-70.

Karthikeyan G, Pius A, Alagumuthu G. 2005. Fluoride adsorption studies of montmorillonite clay. *Indian Journal of Chemical Technology* **12**: 263–272.

Kau PMH, Smith DW, Binning P. 1998. Experimental sorption of fluoride by kaolinite and bentonite. *Geoderma* **84**: 89-108.

Keren R, Sparks DL. 1994. Effect of pH and ionic strength on boron adsorption by pyrophyllite. *Soil Science Society of America Journal* **58**: 1095–1100.

Lipson SM, Stotzky G. 1982. Adsorption of reovirus to clay minerals: effects of cation-exchange capacity, cation saturation, and surface area. *Applied and Environmental Microbiology* **46**: 673–682.

Lipson SM, Stotzky G. 1985. Infectivity of reovirus adsorbed to homoionic and mixed-cation clays. *Water Research* **19**: 227–234.

Ma W, Zhao N, Yang G, Tian L, Wang R. 2011. Removal of fluoride ions from aqueous solution by the calcination product of Mg-Al-Fe hydrotalcite-like

compound. *Desalination* **268**: 20-26.

Mathialagan T, Viraraghavan T. 2003. Adsorption of cadmium from aqueous solutions by vermiculite. *Separation Science and Technology* **38**: 57-76.

Meenakshi S, Sundaram CS, Sukumar R. 2008. Enhanced fluoride sorption by mechnocheminally activated kaolinites. *Journal of Hazardous Materials* **153**: 164-172.

Moore RS, Taylor DH, Reddy MMM, Sturman LS. 1982. Adsorption of reovirus by minerals and soils. *Applied and Environmental Microbiology* **44**: 852–859.

Moore RS., Taylor DH., Sturman LS., Reddy MM., Fuhs GW. 1981. Poliovirus adsorption by 34 minerals and soils. *Applied and Environmental Microbiology* **42**: 963–975.

Park JA, Lee CG, Kim JH, Kang JK, Lee I, Kim SB. 2011. Removal of bacteriophage MS2 from aqueous solution using Mg-Fe layered double hydroxides. *Journal of Environmental Science and Health, Part A* **46**: 1683-1689.

Prasada M, Saxena S. 2008. Attenuation of divalent toxic metal ions using natural sericitic pyrophyllite. *Journal of Environmental Management* **88**: 1273–1279.

Saxena S, Prasad M, Amritphale SS, Chandra N. 2001. Adsorption of cyanide from aqueous solutions at pyrophyllite surface. *Seperation and Purification Technology* **24**: 263–270.

Schiffenbauer M, Stotzky G. 1982. Adsorption of coliphages T1 and T7 to clay minerals. *Applied and Environmental Microbiology* **43**: 590–596.

Schiffenbauer M, Stotzky G. 1983. Adsorption of coliphages T1 and T7 to host and non-host microbes and to clay minerals. *Current Microbiology* **8**: 245–249.

Sobsey MD, Dean CH, Knuckles ME, Wagner RA. 1980. Interactions and survival of enteric viruses in soil materials. *Applied and Environmental Microbiology* **40**: 92–101.

Sobsey MD, Hall RM, Hazard RL. 1995. Comparative reductions of hepatitis A virus, enteroviruses and coliphage MS2 in miniature soil columns. *Water*

Science and Techology **31**: 203-209.

Sobsey MD, Shields PA, Hauchman FH, Hazard RL, Caton LW. III. 1986. Survival and transport of hepatitis A virus in soils, groundwater and wastewater. *Water Science and Techology* **18**: 97–106.

Srinivasan R.. 2011. Advances in application of natural clay and its composites in removal of biological, organic, and inorganic contaminants from drinking water. *Advances in Materials Science and Engineering* **2011**: 1-17.

Sykes IK, Williams ST. 1978. Interactions of actinophage and clays. *Journal of General Microbiology* **108**: 97-102.

Syngouna VI, Chrusikopoulos CV. 2010. Interaction between viruses and clays in static and dynamic batch systems. *Environmental Science and Technology* **44**: 4539-4544.

Taylor DH, Bellamy AR, Wilson AT. 1980. Interaction of bacteriophage r17 and reovirus type III with the clay mineral allophane. *Water research* **14**: 339-346.

Thakre D, Rayalu S, Kawade R, Meshram S, Subrt J, Labhsetwar. 2010. Magnesium incorporated bentonite clay for defluoridation of drinking water. *Journal of Hazardous Materials* **180**: 122-130.

VanDuin J.. 1988. The single-stranded RNA bacteriophages, In R. Calendar(ed.), The bacteriophages, Plenum Press, New York, USA.

Yates MV, Gerba CP, Kelley LM. 1985. Virus persistence in groundwater. *Applied and Evironmental Microbiology* **49**: 778-781.

Zerda KS.. 1982. Adsorption of viruses to charge-modified silica. Ph.D. dissertation, Baylor College of Medicine, Houston, Texas, USA.

Zhang J, Xie S, Ho YS. 2009. Removal of fluoride ions from aqueous solution using modified attapulgite as adsorbent. *Journal of Hazardous Materials* **165**: 218-222.

국문초록

본 연구의 목적은 납석을 흡착제로서 이용하여 수용액상의 불소와 박테리오파지를 제거하는 것이다. 실험에 사용된 납석은 흰색을 띠며 거칠고 불규칙적인 형태의 표면을 갖는다. X선 형광분석 결과 납석의 주요 성분은 Si (74.03%) 와 Al (21.20%) 이었으며 X선 분말 회절 분석에 의하여 석영 (SiO_2), 딕카이트 ($Al_2Si_2O_5(OH)_4$), 납석 ($Al_2Si_2O_5(OH)_4$)으로 구성되어 있음을 확인하였다. FTIR 분광 분석을 통해 수산화기의 존재를 확인하였으며 질소가스 흡탈착법을 이용하여 분석한 결과 납석의 비표면적은 1.3419 m^2/g, 공극의 총 부피는 5.74×10^{-4} cm^3/g 이었으며 공극의 평균 크기는 1.7122 nm 였다.

평형 배치 실험 결과 납석의 불소 최대 흡착량은 0.737 mg/g 이었으며 동역학적 배치 실험 결과 24시간 이내에 평형에 도달하였다. 25−45℃ 범위에서 열역학적 실험을 수행한 결과 납석의 불소 흡착 과정은 흡열반응을 나타내었으며, pH 4.0−9.0 범위에서는 pH의 영향을 거의 받지 않았다. 경쟁음이온의 영향을 살펴본 결과 SO_4^{2-}, HPO_4^{2-}, CO_3^{2-}는 납석의 불소 흡착을 방해하였으나 NO_3^-와 Cl^-는 거의 영향을 끼치지 않았다. 또한 다양한 온도(미처리, 400, 600, 800, 1000, 1100℃)에서 납석을 열처리한 결과 400℃로 열처리할 경우 열처리하지 않은 납석에 비하여 21% 향상된 불소 흡착량을 나타내었다.

MS2를 이용하여 배치실험을 수행한 결과 MS2 초기농도가 2.85×10^6 pfu/mL일 때 30mL의 용액에 대하여 주입된 납석의

양이 0.01g에서 2.0g으로 증가함에 따라 MS2의 제거율이 5.26%에서 99.99%로 증가하였으며 최대 흡착량은 5.01×10^{8} pfu/g 이었다. 동역학적 배치실험 결과 납석에 의한 MS2 제거는 빠르게 이루어지며, 30분 이내에 3.7 log removal, 180분 이내에는 4 log removal 이상의 제거율을 나타내었다. 납석의 MS2 제거에 미치는 불소 이온의 영향을 알아보기 위하여 배치실험을 수행한 결과 불소의 농도가 5 mg/L일 때와 10 mg/L일 때 MS2의 제거율은 각각 3.05 log removal, 2.54 log removal 로서 불소 이온이 존재하지 않는 경우(4.0 log removal)에 비하여 감소하였다. 이러한 제거율의 차이는 납석 표면의 흡착사이트 경쟁에 의해 불소이온이 MS2의 흡착을 방해하였기 때문인 것으로 생각된다. 유량 0.5 mL/min, 초기 MS2 농도 5.98×10^{5} pfu/mL의 조건에서 칼럼실험을 수행한 결과 5 mg/L의 불소 이온이 동시에 존재하는 경우 MS2 흡착량은 4.70×10^{6} pfu/g으로 불소 이온이 존재하지 않는 경우(8.17×10^{6} pfu/g)에 비하여 감소하였으며 칼럼실험에서의 MS2 흡착량의 감소는 배치실험의 결과에 비해 적게 나타났다. 본 연구결과를 통하여 수중의 불소와 바이러스를 제거하는 흡착제로서 납석의 적용 가능성을 확인할 수 있었다.

주요어: 흡착제, 박테리오파지 MS2, 배치실험, 점토, 칼럼실험, 불소, 납석, 흡착, 열역학적 실험

학 번: 2010-23436